Modelling plastic additive release in aquatic environments to support plastic environmental risk assessment

RESEARCH PROJECT

Master Toxicology and Environmental Health

Major Research Project

-

TNO | Innovation for Life

Circularity and Sustainability Impact

Andrea Rujas Arranz

Daily supervisor: Anna Schwarz[1]
Supervisor: Milad Golkaram[1]
Examiner: Hanna Duzsa[2]

[1]Circularity and Sustainability Impact group. Nederlandse Organisatie voor Toegepast Natuurwetenschappelijk Onderzoek (TNO), Utrecht, The Netherlands.
[2]One Health Toxicology, Institute for Risk Assessment Sciences (IRAS), Faculty of Veterinary Medicine, Utrecht University, Utrecht, The Netherlands.

INDEX

ABSTRACT

Plastic litter is reckoned as an issue of global concern due to its prevalent and ubiquitous nature and its detrimental impact on wildlife and ecosystems. One of the ways by which plastic is hypothesized to cause harm to the environment is through the release of potentially toxic additives.

To date, numerous plastic additives are known toxic to human health and the environment. However, most environmental risk assessment (ERA) studies and regulatory frameworks do not consider plastic additives and their release, leading to a biased and incomplete understanding of the ecological implications of plastic pollution. This stems from the lack of accurate and complex mathematical tools that represent the complexity of additive release kinetics and the numerous factors implicated. Addressing this gap, this study introduces an Additive Release Model (ARM), designed to estimate additive losses from plastic litter in aquatic environments. The ARM is intended to implement existing models on plastic accumulation and distribution in the environment, allowing a more complete and realistic Plastic Environmental Risk Assessment.

In the designed ARM, Fick's second law was used as the core equation of the model and two consecutive steps were considered, namely internal and external additive diffusion. The factors temperature, time, water presence, additive molecular weight (MW), polymer type, and polymer size were included. To overcome limitations in input data availability, the Piringer Equation was included in the model to estimate worst-case scenario additive Diffusion Coefficients (D*p). This model was then used to investigate the release of decabromodiphenyl ether (decaBDE), octabromodiphenyl ether (octaBDE), pentabromodiphenyl ether (pentaBDE), and 1,2-Bis(2,4,6-tribromophenoxy)ethane (BTBPE) from Acrylonitrile Butadiene Styrene (ABS), High Impact Polystyrene (HIPS), Polypropylene (PP), and Polyamide (PA) polymers. These additives and polymers are commonly found in old and recycled Electronic and Electrical Equipment (EEE) devices. To validate the ARM and its output, we introduced a positive control. This control was used to compare the ARM's predictions with empirical measurements of additive release and diffusion coefficients (Dp) reported in the literature.

The ARM proved to be a reliable tool for replicating trends in additive release, particularly under internally-controlled diffusivity and using empirically estimated diffusion coefficients (Dp). In line with previous literature, the ARM modeled cumulative additive release over time and release rates escalating with temperature. Notably, low-molecular-weight additives, such as pentaBDE and BTBPE, exhibited the highest release indices from every polymer, irrespective of conditions. Consistent with other studies, a direct correlation was observed between polymer type, additive diffusivity, and additive release, with more amorphous polymers demonstrating higher release rates. However, the reliability of our input dataset came into question due to the inaccuracy of certain assumptions introduced to overcome the scarcity of input data. Nevertheless, the author was aware of the uncertainties and evaluated the output accordingly.

To conclude, the ARM developed in this study represents a preliminary valuable tool to estimate additive release from amorphous polymers. It marks a significant step towards a more comprehensive plastic environmental risk assessment (ERA). Yet, further research is needed to increase the complexity and reliability of the ARM

LAYMAN SUMMARY

Plastic serves society in many beneficial ways. Its affordable, versatile, durable, and lightweight nature explains the increasing demand for this material. Looking ahead, plastic production and use are expected to increase in the coming years. However, plastic also is considered a global environmental concern as large quantities of plastic items are lost in the environment each year. Once in the environment, plastics can harm wildlife, ecosystems, and the quality of natural resources that society relies on.

One of the ways by which plastics are known to be harmful to the environment and human health is through the release of chemical additives from plastic materials. Additive release refers to the leaching of additives from plastic materials into the surrounding environment, including water, soil, food, and organisms. These chemical additives are crucial for achieving specific functional properties in plastics. For instance, certain chemical additives can enhance plastic's flexibility, durability, or resistance. Nonetheless, many of these chemicals are toxic, and, once released, they become available and potentially hazardous,

Additive's release is affected by the physicochemical characteristics of the plastics and the additive chemicals (e.g. different in size, solubility, volatility) and by the different environmental conditions (e.g. exposure to ultraviolet (UV) light, microbial degradation). As it is a complex chemical process, not many studies on plastics' environmental impact include additives and their release. To cover that gap and aid with the implementation of plastic pollution studies, the purpose of this study is to develop an Additive Release Model (ARM), a mathematical model designed to estimate additive losses from plastic litter in aquatic environments. Mathematical models are useful tools that translate real-world systems (i.e. the release of additive chemicals from plastic materials) into mathematical equations and correlations.

Our ARM proved to be a reliable tool to mirror trends in additive release under specific conditions when using empirically estimated input data on Diffusion Coefficients. It accurately modeled cumulative additive release over time, with release rates increasing with temperature. Notably, low-molecular-weight additives (i.e. the chemicals pentaBDE and BTBPE) exhibited the highest release indices from every polymer under any given condition. Consistent with existing literature, a direct correlation was observed between polymer type, additive diffusivity, and additive release, with more amorphous polymers showing higher release rates. However, the criteria for collecting the input dataset must be implemented.

Despite further research is needed to increase the complexity and reliability of the model, our ARM represents a valuable tool for estimating additive release from flexible and amorphous plastic materials. This model marks a significant step towards a more complete and reliable plastic environmental risk assessment (ERA).

ABBREVIATIONS

ABS – Acrylonitrile Butadiene Styrene

ADM – Accumulation and Distribution Model

ARM – Additive Release Model

BPA – Bisphenol A

BTBPE – 1,2-Bis(2,4,6-tribromophenoxy)ethane

BzBP – Benzylbutyl phthalate

DEHP – Bis(2-ethylhexyl) phthalate

DEP – Diethyl phthalate

decaBDE (BDE-209) – Decabromodiphenyl ether

DiBP – Di-isobutyl phthalate

DMP – Dimethyl phthalate

DnBP – Di-n-butyl phthalate

DPP – Dipropyl phthalate

EEE – Electronic and Electrical Equipment

HIPS – High Impact Polystyrene

MW – (additive) Molecular Weight

octaBDE – Octabromodiphenyl ether

PA – Polyamide

PAHs – Polycyclic Aromatic Hydrocarbons

PBCs – Polychlorinated biphenyls

PBDEs – Polybrominated diphenyl ethers

pentaBDE – Pentabromodiphenyl ether

PE – Polyethylene (PE)

PP – Polypropylene

PVC – Polyvinylchloride (PVC)

TCPP – Tris(1-chloro-2-propyl) phosphate

INTRODUCTION

Plastic materials are synthetic organic polymers made of repeating monomer units. Plastic polymers' light, durable, multipurpose, and inexpensive nature explains the increasing popularity and demand for these materials (Andrady & Neal, 2009; Filho et al., 2021). Indeed, since the start of mass plastic consumption in the 1950s, plastic use and production have increased exponentially (UN Environment Program, 2016). In 2018, global plastic production reached 359 million tonnes (Plastics Europe., 2022). Looking ahead, plastic production is expected to reach ca. 1800 million tonnes in 2050 (UN Environment Program, 2016).

In addition, plastics also contain a wide variety of chemical additives. Such additives are intentionally embedded in the primary polymeric matrix to maintain, enhance, and achieve specific and valuable properties. This includes, for example, improving flexibility, preventing adhesion, reducing flammability, and preventing heat deterioration and oxidation. Furthermore, processing aids that ease and enable the production and processing of polymers can also be found in plastic materials. Beyond these intentionally added chemicals, non-intentionally added substances (NIASs) such as byproducts, contaminants, and breakdown products are also commonly present (Barrick et al., 2021; Bridson et al., 2021; Wiesinger et al., 2021).

Plastic has been highlighted as an issue of global concern due to its prevalent and ubiquitous nature and its detrimental impact on wildlife and ecosystems (European Environment Agency, 2023; Lambert & Wagner, 2017). The systematic loss of plastic products into the environment at every stage of their life cycle has led to plastic accumulation in various environmental compartments (Gallo et al., 2018; Groh et al., 2019). The uptrend in plastic demand, production, and use is expected to aggravate plastic environmental pollution and its associated impact. Indeed, global emissions were modeled to 8.7 million tonnes (mt) for macroplastics and 0.8 mt for microplastics in 2017 (Schwarz et al., 2023). By 2050, macro and microplastic emissions are expected to reach 2.2 gigatonnes (Gt) and 3.1 Gt, respectively, under the business-as-usual scenario (Schwarz et al., 2023). To tackle the environmental impact of plastic litter, it is essential to predict the environmental fate and concentration of plastics in different environmental compartments. To that aim, several mathematical models have been developed (Sheela et al., 2022; Uzun et al., 2022a). Such mathematical models integrate the various transport, transformation, and (bio)degradation processes that ultimately determine the environmental occurrence of plastic litter. For instance, Material Flow Analysis (MFA) models have been used to estimate the emissions of macro and microplastics into the environment from the plastic value chain and into multiple environmental compartments. This type of approach allows the prediction of plastic emissions into aquatic and terrestrial ecosystems from different industrial sectors and the accumulation patterns at the regional and global scale (Kawecki & Nowack, 2019; Schwarz et al., 2023).

Yet, the environmental impact of plastic litter goes beyond its accumulation in natural and anthropic environments. One of the ways by which plastic litter is hypothesized to be harmful to the environment is through the release of plastic additives. While embedded in the polymer matrix, additives pose no or limited toxicity due to their low bioavailability and reduced mobility (Viljoen et al., 2023). However, most additives are not chemically bound to the polymer matrix, they can be easily released from the polymer matrix through migration and leaching processes, under certain conditions, and at every stage of the plastics life cycle (Barrick et al., 2021; Bridson et al., 2023; Hahladakis et al., 2018; Luo et al., 2022). Additive release has been often reported for plastics in use, with packaging materials being extensively studied (Groh et al., 2019). Additionally, recent studies have shown an increase in the additive release rate following plastic littering into the environment. In most cases, such increase is explained by aging processes, such as degradation and fragmentation, endured by plastic

materials, which alter the initial additive-polymer configuration, facilitating additive loss (Hahladakis et al., 2018; H. Liu et al., 2020; Paluselli et al., 2019; Teuten et al., 2009). Several studies have delved into the adverse environmental and health effects associated with plastic-related additives, with some reporting potentially toxic additive concentrations in ecological compartments (Chen et al., 2023; Fauser et al., 2022; He et al., 2015; Tang et al., 2015, 2016; L. Zhang et al., 2015). Hence, the environmental risk posed by plastic depends not only on the occurrence and accumulation of plastic polymers themselves but also on the release of potentially toxic additives.

However, despite the growing scientific evidence and concern about the environmental toxicity of plastic additives, most impact assessment studies either do not consider plastic additives or are solely focused on a selection of well-known and frequently used chemicals (Bergmann et al., 2022; Lebreton et al., 2018; Martin et al., 2017; Matsuguma et al., 2017; Napper et al., 2020; Nawab et al., 2023). The scarce inclusion of additive chemicals is also evident in many current circularity initiatives and regulatory actions (Hahladakis et al., 2018; Stenmarck et al., 2017; Wiesinger et al., 2021). Such a trend may account for the limited, scattered, and heterogeneous information on plastic additives, non-harmonized regulations, and the rapid incorporation of new chemicals into the market (Aurisano et al., 2021; Groh et al., 2019; Wiesinger et al., 2021). In addition, the complexity of additive release kinetics and the numerous factors implicated have likewise hindered the development of theoretical models to estimate additive losses.

Aiming to set a reliable groundwork to assess the release of additives and the related risks to human health and the environment, several mathematical approaches have been progressively developed over the last decades. However, most of them are tailored to additive release from food-contact materials and into food, with no or limited application at the environmental level (Douziech et al., 2020; Petrosino et al., 2023; Poças et al., 2012; Reynier et al., 2002; Uzun et al., 2022). To date, only a few studies have developed theoretical models focused on additive release from plastic litter accumulated in ecological compartments. However, these studies are coupled with experimental techniques such as passive migration experiments (Feng, 2020; Lee et al., 2018; Sun et al., 2019). Therefore, their reliance on empirical estimations limits their applicability and combination with existing models on plastic accumulation and distribution.

RESEARCH FOCUS AND PROJECT OUTLINE

This study aims to lay the foundations of a first additive release model (ARM) to estimate additive losses out of plastic litter in environmental compartments. Our mathematical model is intended to implement existing ADM models, allowing a more complete and realistic Plastic Environmental Risk Assessment.

The thesis begins by establishing a theoretical framework. This framework was built based on a preliminary literature review and aims to outline the steps involved in additive release kinetics, as well as the environmental and physicochemical factors that influence additive loss. The theoretical framework served as our first conceptual model, which was later translated into a set of algorithms, assumptions, and correlations, resulting in our ARM.

Subsequently, a set of well-defined PBDE additives was selected based on their environmental toxicity and data availability, and a thoughtful input data collection was performed. Next, the ARM was used to estimate PBDE release from four polymers commonly used in the Electronic and Electrical Equipment (EEE) sector as a first proof of concept. To demonstrate the validity of the ARM, a positive control was likewise introduced to validate the ARM output against empirical measurements on additive release rate.

METHODOLOGY

PART 1. MODEL DEVELOPMENT

To establish the groundwork for the Additive Release Model (ARM), a conceptual model was constructed based on an initial literature review. The conceptual model delineates a set of well-defined environmental and physicochemical factors and provides an overview of additive release kinetics. Based on this foundation, the mathematical model was designed. Existing mathematical models on additive release in the water phase and from food-contact materials were considered as a reference and the boundary conditions were adapted to aquatic environments. The ARM was designed in Excel Office 16 and Mathematica v.14.

1.1. The conceptual model

Conceptual models represent the set of assumptions, ideas, theories, variables, and relationships between the different variables controlling the behavior of a system. The conceptual model presented here summarizes the current understanding of additive release kinetics along with a set of physicochemical and environmental factors governing additive release rate behavior. This theoretical model was translated into algorithms, assumptions, dependent and independent variables, and correlations between the different environmental and physicochemical factors to build the ARM.

To obtain a generic overview of (*i*) the different environmental and physicochemical factors governing additive release, and *(ii)* additive release kinetics, a preliminary literature review was performed. The databases PubMed, Scopus, and Google Scholar were used for the search.

The search items used to explore the physicochemical and environmental factors were *plastic additives* and *additive release*, together with *aquatic environments, ocean, inland water, freshwater, environmental fate, toxicity, bioavailability, environmental conditions,* and *desorption*. To study additive release kinetics, search items used were *plastic additives migration kinetics* or *plastic additive release kinetics* or *plastic additive desorption kinetics*, together with *food-contact materials* or *aquatic environments* or *mathematical models.*

Based on reviewed primary articles and systematic reviews, the abovementioned search items were truncated, explored, and adjusted to achieve optimal results. In addition, manual searches of reference lists of relevant articles were carried out to identify further studies.

Environmental and physicochemical factors influencing additive release

Additive mobilization and release from polymers are simultaneously governed by numerous physicochemical and environmental factors, as presented in Table 1. Despite the heterogeneity of the studies, an overall intertwined solid correlation between both types of factors is commonly reported regardless of the type of polymer, additive, and environmental compartment. The revised literature, together with the factors evaluated per study, can be found in Annex 1.

The physicochemical factors polymer size and polymer crystallinity, additive molecular weight (MW), and additive hydrophobicity were strongly and consistently associated with additive release behavior in the reviewed studies. As a common trend, additive release increases with decreasing polymer size, crystallinity, and additive MW (Allan et al., 2022; Li et al., 2019; H. Liu et al., 2020).

Additive diffusivity and release are hypothesized to vary between polymer types as a function of their polymeric structural disposition and chemical conformation Depending on the disposition, the polymer's structure will range between crystalline and amorphous. More amorphous polymers present random chemical conformations and spaces between polymeric chains. As a result, amorphous polymers are flexible at low temperatures and additives are expected to diffuse easily through them (Allan et al., 2022; Askadskii et al., 2014; Petrovics et al., 2023). Additive hydrophobicity determines the desorption kinetics of additives from the polymeric surface and into the nature of the surrounding environment (i.e. aquatic environment vs soil-based ecosystems). Such property is usually expressed as the octanol-water partitioning coefficient (Kow) or the plastic-water partitioning coefficient (Kpw) (Allan et al., 2022; Lee et al., 2018; Li et al., 2019; Town & Van Leeuwen, 2020).

Table 1. Overview of the different factors and parameters affecting additive release behavior. The number of reviewed studies addressing each factor is also presented. The factors are classified as (a) physicochemical factors relative to the polymer and additive, (b) environmental factors, and (c) aging effect. The aging effect results from the combination of the exposure of polymers with given physicochemical properties to a set of environmental factors over time.

Factor	Number of studies (N)	Ref #
Physicochemical factor		
Polymer size	10	1, 2, 3, 4, 6, 8, 9, 11, 14, 16
Polymer type	7	1, 2, 9, 11, 16, 15, 17
Additive MW	6	1, 3, 9, 16, 18, 19
Additive hydrophobicity	5	4, 8, 13, 15, 16
Environmental factor		
Time	6	3, 9, 11, 12, 18, 19
Temperature	8	6, 7, 9, 10, 11, 12, 18, 19
Water content (w %)	5	1, 5, 6, 14, 18
UV light exposure	8	1, 2, 4, 5, 6, 7, 11, 19
Organic matter content (OM%)	3	4, 7, 19
Microbial activity	3	1, 6, 14
Organisms intake	3	8, 12, 13
Hydrostatic pressure	1	14
pH	4	7, 8, 10, 15
Ageing processes	2	1, 12

Natural factors such as ultraviolet (UV) light exposure, microbial enzymatic activity, and additive mobilization upon organisms´ intake were positively associated with increased additive release (Bakir et al., 2014; Fauvelle et al., 2021; Hirai et al., 2011; Li et al., 2019; H. Liu et al., 2020; Paluselli et al., 2019). Aging processes undergone by plastic materials over time are commonly referred to as one of the main enhancers of additive release, reflecting the intertwined association between environmental and physicochemical factors (H. Liu et al., 2020; Luo et al., 2022; Paluselli et al., 2019). Such an aging effect is understood as the alteration of the physicochemical nature of plastic materials and embedded additives over time and due to the exposure to environmental stressors (e.g. high temperatures or prolonged UV light exposure) resulting in polymer fragmentation, changes in the inherent initial properties, and the alteration of additive release rate. For simplification, while maintaining accuracy,

only the parameters presented in Table 2 were considered in our model. The selected parameters had a well-defined correlation with additive release behavior.

Table 2. Environmental and physicochemical factors were selected to be included in the ARM. The right column displays the factor correlation with additive release behavior (i.e. [-] Decrease, [+] Increase).

FACTOR	CORRELATION
Polymer size	**[-] Polymer size >** [+] Additive release
Polymer crystallinity	**[-] Polymer crystallinity >** [+] Additive release
Additive molecular weight (MW)	**[-] Additive MW >** [+] Additive release
Additive hydrophobicity and hydrophilicity (Kow)	**[+] Hydrophobicity >** [-] Additive release *
Time	**[+] Time >** [+] Additive release
Temperature	**[+] Temperatura >** [+] Additive release
Water presence	Strong dependency on additive hydrophobicity

** Strong dependency on water and organic matter presence in the surrounding environment*

Additive release kinetics

Additive release from the polymeric matrix occurs via mass transport mechanisms and desorption processes via two consecutive steps depicted in Figure 1, inner additive diffusion through the polymeric matrix or Step 1; and additive desorption from the polymeric surface and diffusion polymer-water boundary layer or Step 2 (Allan et al., 2022; Feng, 2020; Sun et al., 2019).

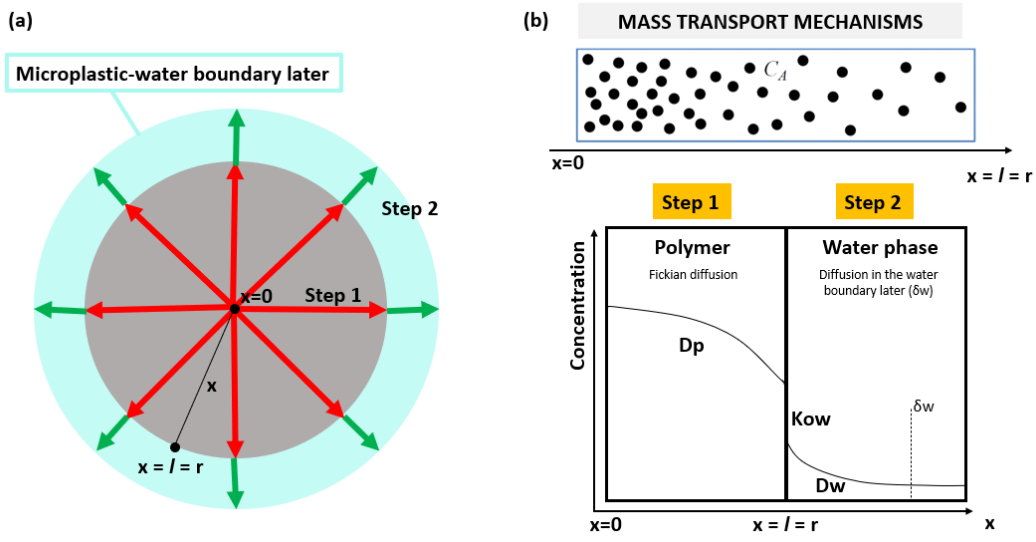

Figure 1. Primary mass transfer and desorption steps and physicochemical parameters involved in additive diffusion and release from spherical MNPs in the water phase: (a) Graphical illustration of additive radial diffusion and release from spherical MNPs; (b) additive diffusivity is explained by mass transport mechanisms where particles movement is driven by a difference in concentration gradient within the system. In Step 1, internal additive diffusion is explained by Fick's second law and governed by the additive Diffusion Coefficient (Dp). In Step 2, additive desorption from the polymeric surface and external additive diffusion is controlled by the additive partitioning coefficient (Kow) and additive diffusivity in the water phase (Dw), respectively.

The mass transport mechanism of a diffusive solvent (i.e. the additive species) through porous membranes (i.e. the polymer) is driven by the difference in species concentration at different locations

within the system. That is, additives embedded in the plastic matrix diffuse towards the polymer surface driven by a negative difference in concentration (i.e. from a highly concentrated inner bulk to the less concentrated polymer surface) (Figure 1). Once in the surface, additives will desorpt from the polymer surface and into the surrounding polymer-water boundary layer. The additive desorption rate is determined by additive hydrophobicity, expressed as Kow (Kwon et al., 2017; Lee et al., 2018). The internal negative concentration gradient will increase from additive desorption, enhancing additive mobilization from the inner matrix (Paluselli et al., 2019).

Additive diffusion and release will continue until the equilibrium with the surrounding environment is reached. However, when the volume of the surrounding environment is relatively "infinite" - as it is assumed under environmental conditions - the additive release process undergoes an unsteady-state circumstance until the entire volume of additives is released (Karimi, 2011; Lee et al., 2018; Sun et al., 2019). Fick's second law can explain such unsteady-state mass transfer circumstance**:**

$$\frac{\partial C}{\partial t} = D\frac{\partial^2 C}{\partial x^2} \qquad Equation\ (1)$$

Collected literature on additive release kinetics, mass transport mechanisms, and existing mathematical models on additive release kinetics can be found in Annex 2.

1.2. Model design

Based on the previously described theoretical foundation, a set of assumptions, algorithms, and relationships between the different environmental and physicochemical factors were delineated. This groundwork was used to build the ARM. A simplified model overview is presented in Figure 2 below. The complete mathematical model can be found in the Supplementary Excel.

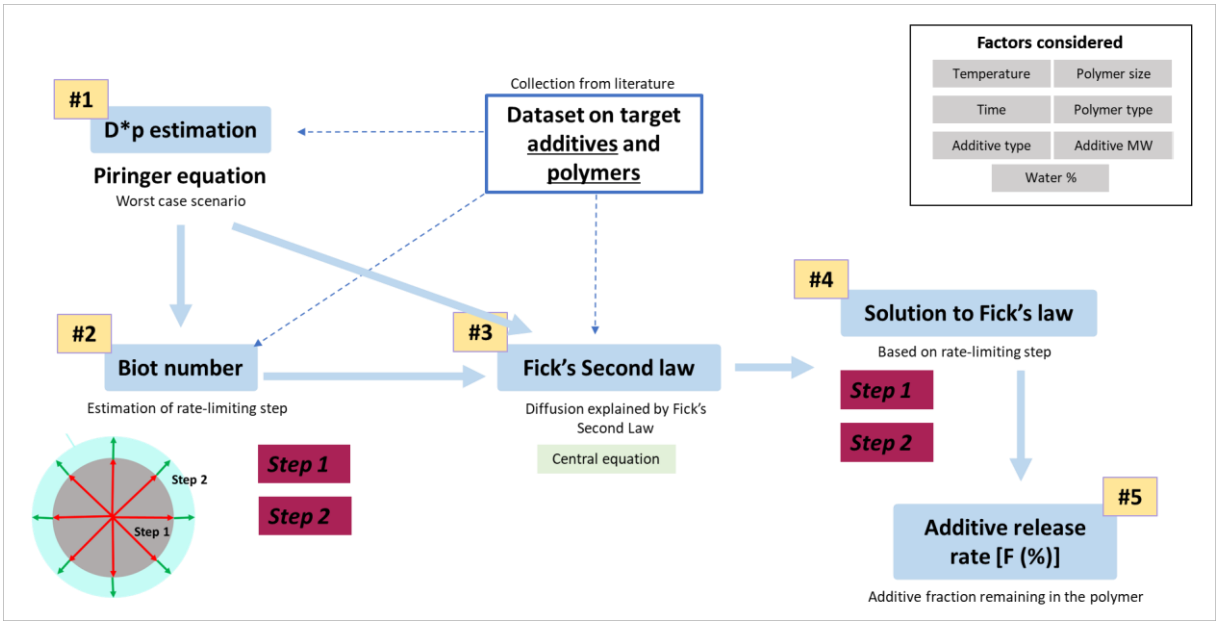

Figure 2. Simplified overview of the ARM workflow.

Fick's second law

Existing additive migration models are based on mass transport mechanisms where chemical diffusion and release are controlled by the diffusion coefficient (D) and partitioning coefficient (Kow) at a given time (t) and temperature (T) range. By combining these factors, the unsteady-state additive diffusion process can be explained by Fick's second Law (Eq. 1) (Costa et al., 2023; Dong & Gijsman, 2010; Feng, 2020; Karimi, 2011; Lee et al., 2018):

$$\frac{\partial C}{\partial t} = D\frac{\partial^2 C}{\partial x^2} \qquad Equation\ (1)$$

where C is the total concentration of additives, D is the diffusion coefficient of additives transport through the polymeric matrix, and x (or r for radial/spherical particles) is the distance from the center of the particle.

Assuming a spherical structure of MNP polymers and that additives will diffuse radially, Equation (1) takes the form of Equation (2):

$$\frac{\partial C}{\partial t} = D\left(\frac{\partial^2 C}{\partial r^2} + \frac{2}{r}\frac{\partial C}{\partial t}\right) \qquad Equation\ (2)$$

Assumptions for the model and boundary conditions

Several assumptions are taken in this project to estimate additive release under standard conditions:

1. Plastic particles have a spherical shape, and the surface remains intact.
2. Plastic composition is homogeneous and isotropic.
3. Plastic particle size is in the range of micro and nanoplastics (MNPs). MNPs sized 1 µm and 500 µm are considered. MNPs do not degrade further over time.
4. The additive is uniformly distributed inside the plastic. The initial maximum concentration in MNPs (C_0) will equal that of polymers after production.
5. The additive will diffuse radially within the polymer.
6. The thickness of the microplastic-water boundary layer (δw) is equal to half of the thickness of the plastic (l).
7. The surrounding environment is considered an "infinite sink" with a constant volume. As the environment has a continuous infinite volume, the diffusion coefficient is an unsteady-state circumstance.
8. No environmental pollutants are sorpted to the MNP surface. The only chemicals present on the MNP surface are those inherent to the polymer.
9. The environment is stagnant so the influence of turbulence is neglected. Other factors inherent to aquatic environments, such as changes in hydrostatic pressure or UV light exposure are likewise neglected. Only the environmental factor temperature (T) will directly enhance or diminish additive release over time (t).

By appliying these assumptions, the model boundary conditions, and initial condition were set to:

- $C = C_0$, $0 < x < l$, $t=0$
- $C = C_0$, $x = 0$, $t \geq 0$
- $J = -D\left(\frac{dC}{dx}\right) = k\,(C0 - Cs), x = l, t \geq 0$.

Where *l* is half of the thickness of the plastic. Therefore, given that the MNP is spherical: *l = r (radius).* The parameter x refers to any point in the sphere between the center (x=0) and the surface of the sphere (x=*l*=*r*), and *k* is the mass transfer coefficient (Figure 3).

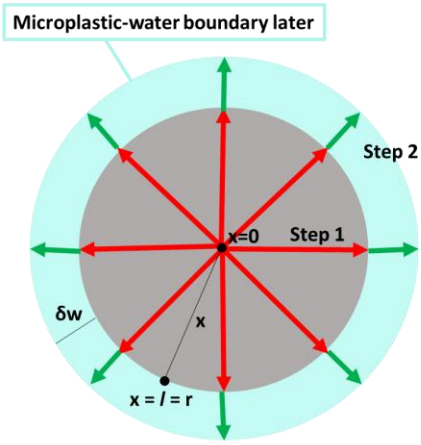

Figure 3. Graphical illustration of additive radial diffusion and release from spherical MNPs in aquatic environments.

Diffusion Coefficient Estimations

Empirically, Dp values are obtained using passive sampling experiments performed at a given temperature and over time (Allan et al., 2022; Kruczek, 2015; Lee et al., 2018; Sun et al., 2019; Town & Van Leeuwen, 2020). However, given the limited available data on experimentally determined diffusion coefficients in plastics (*Dp*), the worst-case diffusion coefficients (D*p) were derived from the Piringer equation (Eq. 3) to complete our dataset. A similar approach was previously used in literature, (Hamdani et al., 1997; Limm & Hollifield, 1996; Nguyen et al., 2013a; Piringer, 1994; Plastics Europe, 2021).

D*p is a polymer-specific upper-bound diffusion coefficient. Thereby, as D*p ≥ Dp, it must be emphasized that using D*p leads to the *worst-case* additive loss estimations. D*p estimations are a function of temperature (T) and additive molecular weight (MW). Thus, D*p can be calculated for a given additive and temperature range and used instead of Dp.

Piringer equation is enunciated as follows (Equation 3) :

$$D^*p\,(M,T) = \exp\left[A^*p - 0.135MW^{\frac{2}{3}} + 0.003MW - \frac{10454 \cdot \mathrm{R}}{T \cdot \mathrm{R}}\right] in\ m^2 s^{-1} \qquad Equation\ (3)$$

where MW is additive molecular mass, T refers to the absolute temperature (°K), A*p is a temperature-independent and polymer-specific diffusion parameter, and τ is a polymer specific activation energy parameter (°K).

The variables MW and T make D*p values additive- and temperature-dependant. The parameter A*p is polymer-specific and temperature-dependent and describes the basic estimated diffusion behavior of migrants within the polymer. That is, polymers with low crystallinity (e.g. LDPE) present high A*p values, reflecting high diffusion behavior (D*p) and migration rate through the polymer; whereas polymers with a higher degree of crystallinity (e.g. polyesters), lower A*p values led to lower diffusion and migration rates.

A*p values can be empirically obtained by performing kinetic studies where additive migration is measured at certain time points and given temperatures (J.S. Baughan, 2015). Yet, A*p can also be calculated with a mathematical approach used in this study and based on Equation (4), where A'*p is a temperature-independent value, T refers to the absolute temperature (T), and τ to the polymer-specific activation energy (°K). A'*p and τ were collected from Plastics Europe (2021).

$$A^{*}p = A'^{*}p - \frac{\tau}{T} \qquad Equation\ (4)$$

the constant τ describes the activation energy of diffusion (E_A). τ is polymer-specific and obtained by combining τ and 10454 with the gas constant R (R= 8,13145 J/mol/K).

$$E_A = (\tau + 10454\ ) \cdot \mathrm{R} \qquad Equation\ (5)$$

Thereby, by using D*p values, additive migration will be overestimated. Consequently, the model output will provide additive loss worst-case scenario rates within certain temperature ranges.

Biot number

In additive loss rate from polymers, the rate-limiting step (i.e. lower step) can be either the internal or the external diffusivity. The solution to Equation (1) will depend on the rate-limiting step. To estimate which process dominates additive release, the Biot Number (Bi) must be calculated.

The Biot Number is a dimensionless value originally used in heat transfer calculations. When applied to mass diffusion processes in our model, mass transfer Biot Number estimates the ratio between the rate of additive transport at the plastic-environment layer on the surface (i.e. Step 2, external diffusion) to the additive transfer resistance rate within the polymer (i.e. Step 1, internal diffusion) (Tawfik A. Saleh, 2022):

$$Bi_m = \frac{k\ Lc}{Dp} \qquad Equation\ (6)$$

where *k* is the additive mass transfer coefficient in the plastic-water boundary layer. The parameter *k* is a diffusion rate constant that correlates mass transfer area, mass transfer rate, and concentration

change as driving force. Dp refers to the diffusion coefficient within the polymer and Lc refers to the characteristic length. Lc is estimated as the volume of a system divided by its surface, as depicted in Equation (7).

To obtain *Lc* values:

$$Lc = \frac{Vbody}{A\ surface} \qquad Equation\ (7)$$

To obtain *k* values, Equation (8) applies:

$$k = \frac{D_w}{K_{ow}\delta_w} \qquad Equation\ (8)$$

where Dw is the diffusion coefficient in water ($m^2\ s^{-1}$), Kow is the plastic-water partitioning coefficient and δ_w is the thickness of the plastic-water boundary layer. In stagnant aqueous environments, δ_w is assumed as equivalent to the radius of the sphere (δ_w = r = l). According to Bingbing Sun (2019), Dw values can be calculated from the Hayduk-Laudie correlation (Hayduk & Laudie, 1974) as follows:

$$Dw = \frac{13{,}26^{-9}}{\mu^{1,4}\ v_m^{0,589}} \qquad Equation\ (9)$$

where μ refers to the dynamic viscosity of water (Pa · s) and v_m is the LeBas molar volume ($cm^3 \cdot mol^{-1}$). v_m can be calculated from the molecular structure of the diffusan, based on the additive method described by Yahyaee et al. (2018) and depicted in Equation (10). *N* refers to the n number of atoms of Carbon, hydrogen, and oxygen, as indicated by the subscripts *C, H, O*, respectively. *DB* stands for double bonds and 7* is included if diffusants have aromatic rings:

$$v_m = 7(N_c + N_H + N_0 + N_{DB}) + 31{,}5\ N_{Br} - 7^* \qquad Equation\ (10)$$

By combining Equations (6) and (8), Equation (11) can be used to calculate Bi_m.

$$Bi_m = \frac{D_w}{D_p}\frac{1}{K_{ow}}\frac{Lc}{\delta_w} \qquad Equation\ (11)$$

Based on Bi_m values, Fick's second law was solved based on the rate-limiting step. If Bi>1, additive release abides by Case I, in which additive diffusion through the polymeric matrix is the rate-limiting step. In this situation, the rate of additive internal diffusion within the polymer is lower than that of external diffusion. Case II occurs when the Bi value hovers around 1, meaning the rate of both diffusion steps is almost equal. Under this scenario, a careful screening of the ongoing tendency should be performed to apply the most accurate solution to Fick's law. If Bi <1, additive external diffusion is slower, being that the limiting step and Case III would apply (Feng, 2020).

Solutions to Fick's law based on Biot number

Case I (Bi>1, internal diffusion is the rate-limiting step) and Case III (Bi<1, external diffusion is the limiting step) are applied to estimate the ratio between the amount of additives remaining inside plastic matrix (M) to the total amount that can release under an infinite time condition (M_∞). This ratio is indicated as F% and represents the additive fraction (%) remaining in the polymer after a given time.

$$F\ (\%) = \frac{M}{M_\infty} \qquad Equation\ (12)$$

Solution to Case I (Bi > 1, internally-controlled process)

In Case I, Fick's second law was solved based on the initial condition and boundary conditions described by Crank (1975):

a. $C = C_0,\ 0 < x < l,\ t = 0$
b. $C = C_0,\ x = 0,\ t \geq 0$
c. $C = C_s,\ x = l,\ t \geq 0$

Equation (1) can take the form of:

$$C\ (x,t) = \frac{4C_0}{\pi}\sum_{n=0}^{\infty}\frac{1}{2+1}\sin\left[\frac{(2n+1)nx}{l}\right]e^{-\frac{(2n+1)^2\pi^2 D_p}{l^2}t} \qquad Equation\ (13)$$

$$F\ = \frac{M}{M_\infty} = \frac{8}{\pi^2}\sum_{n=0}^{\infty}\frac{1}{(2+1)^2}\exp\left[-(2n+1)^2\pi^2\frac{D_p t}{l^2}\right] \qquad Equation\ (14)$$

For spheres, the resulting equation will take the form of:

$$F = \frac{M}{M_\infty} = \frac{6}{\pi^2}\sum_{n=1}^{\infty}\frac{1}{n^2}\exp\left(-n^2\pi^2\frac{D_p t}{r^2}\right) \qquad Equation\ (15)$$

Solution to Case III (Bi < 1, externally-controlled process)

Assuming this condition in which the rate-limiting step is external diffusion, Fick's second law would be solved as (Feng, 2020):

$$V\frac{\partial C}{\partial t} = A\ k\ (C_s - C_0) \qquad Equation\ (16)$$

Resulting in:

$$F = \frac{M}{M_\infty} = exp\,(-\frac{D_w}{K_{ow}\delta w\, L_c}\, t) \qquad Equation\ (17)$$

where V is the volume, A the surface area and, Lc refers to the characteristic length of the plastic particle.

Estimations of additive released mass fraction [1 – F%]

F% represents the additive fraction remaining in the polymer after a given time by estimating the ratio between the amount of additives remained inside plastic matrix (M) to the total amount that can release under an infinite time condition (M_∞).

$$F\ (\%) = \frac{M}{M_\infty} \qquad Equation\ (12)$$

To obtain the additive fraction released into the environment, a simple estimation was included in the model (Eq. 18). [1 – F (%)] equals the ratio between the additive fraction released over a given period of time (M_t) to the total amount that can release under an infinite time condition (M_∞), as follows:

$$[1 - F\ (\%)] = \frac{M_t}{M_\infty} \qquad Equation\ (18)$$

Environmental and physicochemical factors included in the ARM

The ARM here developed is based on three important environmental factors, namely temperature (T), time (t), water content (W%); and four key physicochemical parameters, that is polymer size (µm), polymer type (i.e. polymer crystallinity), additive molecular weight (MW), additive hydrophobicity (Kow). The selected factors were combined, correlated, and included at different stages of the ARM to reproduce additive release kinetics and factor-determined additive release behavior.

As presented in Figure 4, D*p is obtained as a function of polymer crystallinity (A*p) and additive molecular weight (MW) at a given temperature (T). The Biot number relates polymer size (Lc), water presence (Dw, Kow, δw), polymer type (via D*p), additive MW, and temperature (T). The three latter parameters are indirectly included in the equation via D*p. Case I solution combines time (t), polymer size, polymer type, additive MW, and temperature via Dp. Case II solution considers water presence (Dw, Kow, δw), polymer type (via Kow and Dw), and time (t).

The parameters additive Diffusion Coefficient (D*p) and additive Partitioning Coefficient (17Kow) are essential to additive release kinetics (Figure 1). Such factors have been previously used in

the literature to determine additive release over time, both in empirical and modeling studies (Allan et al., 2022; Kwon et al., 2017; Lee et al., 2018; Town & Van Leeuwen, 2020; Vitrac et al., 2007).

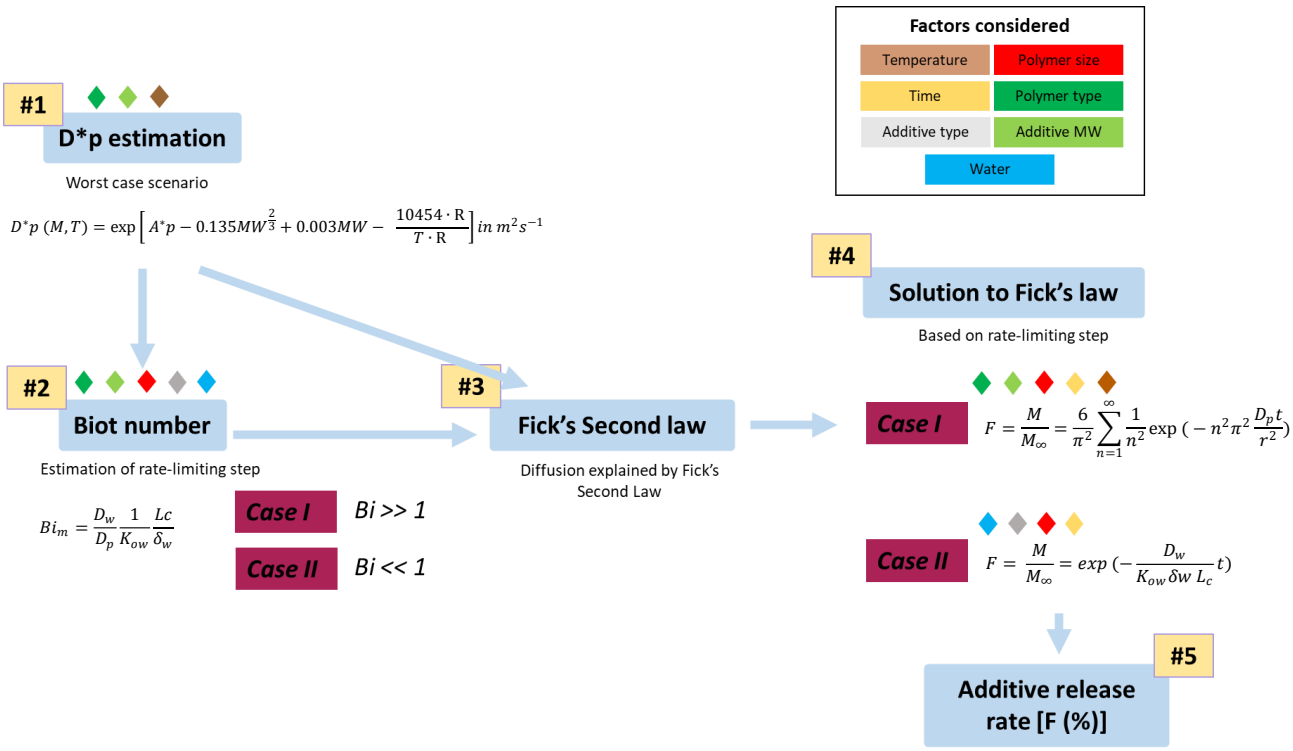

Figure 4. Schematic illustration of the ARM workflow including the main equations. The factors considered in each equation are indicated according to the legend.

PART 2. MODEL APPLICABILITY

In the second stage of this project, the model was applied to estimate the release from Acrylonitrile Butadiene Styrene (ABS), High Impact Polystyrene (HIPS), Polypropylene (PP), and Polyamide (PA) of four well-defined polybrominated diphenyl ethers (PBDEs) commonly used in Electric and Electronic Equipment (EEE). To select the target additives, an initial screening of available literature on additive environmental toxicity was performed. In addition, a positive control was selected and included in the analysis to evaluate the accuracy and reliability of the model.

Upon selection of the target additives, an exhaustive data collection was performed. Next, input data was entered into the model, and additive release was estimated at different conditions of time and temperature. Finally, the model output was screened and compared to those correlations and additive release trends described in the literature.

The complete model workflow can be found in the Supplementary Excel, worksheet *Model workflow overview.*

2.1. The electronic and electrical equipment (EEE) industrial sector and related polybrominated diphenyl ethers (PBDE).

Before additive selection, the classification per industrial sector used in the study by Schwarz et al. (2023) was screened aiming to evaluate the production, consumption and waste management per sector. Next, available literature was examined to evaluate the environmental impact and the additives most commonly used per sector. On this basis, the EEE industrial sector was selected given the high concentrations of environmentally toxic additives found in EEE devices, and the significant environmental accumulation of wasted EEE devices (e-waste) in different regions over the last decades (Mao et al., 2020; J. Wang et al., 2015; K. Zhang et al., 2012; Zheng et al., 2024).

Electronic waste (e-waste) has been recognized as an issue of global environmental concern (Zhang et al., 2012). In 2014, e-waste was recognized as the fastest-growing solid waste stream in the world (International Labour Organization, 2014). Only in 2019, an estimated 53.6 million tons of e-waste were produced globally, but only 17.4% were documented as formally collected and recycled (Forti et al., 2018). According to The United Nations' most recent report on global e-waste monitoring, it is estimated that 74 million metric tons of e-waste will be produced by 2030 (Adrian et al., 2020).

In parallel, e-waste devices are reported to contain large significant concentrations of toxic metals (i.e. lead and cadmium), and toxic additives such as polychlorinated biphenyls (PCBs), Polycyclic Aromatic Hydrocarbons (PAHs) and Polybrominated Diphenyl Ethers (PBDEs), to name but a few (Mao et al., 2020; Tang et al., 2015; K. Zhang et al., 2012). The environmental and human burden of e-waste-related toxicity is particularly concerning in countries that host large e-waste dumping grounds. In countries such as Ghana, China, or Thailand, soil and water have been found to be highly polluted with high levels of toxic chemicals and additives associated to e-waste (Alabi et al., 2021; Awere et al., 2020; Lu et al., 2023; Pibul et al., 2023; J. Wang et al., 2015). For instance, several studies have reported high concentrations of metals and toxic additives such as OPFRs and BFRs in soils from e-waste sites in China, a country that until 2018 was processing 70% of the e-waste worldwide (Lu et al., 2023; J. Wang et al., 2015).

In EEE, plastic material is used in the frame, internal structural parts, functional parts, and internal electronic components for insulation, noise reduction, and sealing (Nnorom & Osibanjo, 2008). Yet, the w/w% (weight by device weight percentage) and type of polymer vary with the type of device and material. ABS and HIPS are the plastics more commonly found in e-waste (da Silva Müller Teixeira et al., 2021; Martinho et al., 2012). Such observation was supported by Mao et al. (2020), who state that ABS, PS, HIPS, and a mixture of PC/ABS are the polymers more present in EEE. In this study, e-waste polymeric composition was based on the summary provided by Kousaiti et al. (2020) (Table 3).

Reducing the flammability of EEE devices is imperative given the extreme operating conditions of some e-components. To this aim, flame retardants (FRs) are widely used to increase resistance to ignition and combustion (Buekens & Yang, 2014).

Among the different FRs formulations, brominated flame retardants (BFRs) are the most powerful group of compounds. BFRs are applied to 2.5M tonnes of polymers annually and the electronic industry accounts for the greatest consumption, followed by building materials and transportation and off-shore vessels (Buekens & Yang, 2014; Ministry of Environment and Food Denmark, 2016). Only in 2016, a Danish project estimated that 70% of used BFRs were contained in EEE devices (Ministry of Environment and Food Denmark, 2016).

Table 3. Typical e-waste polymeric composition adapted from Kousaiti et al. (2020).

Typical e-waste composition		
Polymer	**Acronym**	**w/w (%) in e-waste**
Acrylonitrile Butadiene Styrene	ABS	30%
High Impact Polystyrene	HIPS	25%
Polypropylene	PP	8%
Polycarbonate	PC	10%
PC/ABC	PC/ABS	9%
Polystyrene	PS	3%
Polyamide	PA	3%
Polybutylene terephthalate	PBT	2%
Polyphenyl ether/HIPS	PPE/HIPS	7%

Over decades, a growing body of evidence has shed light on the human and environmental hazards posed by these chemicals, leading to the classification of some of them, such as PBDEs and HBCDDs, as persistent organic pollutants by the UNEP Stockholm Convention. In consequence, BFRs such as PBDEs or PBBs were banned in the 2000s (UN, 2010; Stubbings et al., 2021). PBDEs such as pentaBDE and octaBDE have been banned in the EU since 2004, and decaBDE since July 2008 (Ministry of Environment and Food Denmark, 2016). In consequence, new brominated flame retardants (nBFRs) were introduced in the market as an alternative additive. For instance, the nowadays commonly used BTBPE was introduced as a replacement for octaBDE (de Wit et al., 2010).

However, additives such as PBDEs and PBBs are still present in many day-to-day EEE devices via recycled polymers. Indeed, some studies have revealed substantial concentrations of BFRs in mixed Electrical and electronic waste samples used as the basis of recycled products, particularly in ABS and PS-HIPS polymers (Stubbings et al., 2021). In addition, nBFRs such as BTBPE have been demonstrated to accumulate in the environment and be potentially toxic to human health and the environment (de Wit et al., 2010; Q. Zhang et al., 2023).

2.2. Data collection

Four polybrominated diphenyl ethers (PBDEs) commonly used as brominated flame retardants (BFRs) in the Electrical and Electronic Equipment sector (EEE) were selected, namely pentaBDE, octaBDE, decaBDE, and BTBPE. The selection of PBDEs was done based on the reported additive human and environmental toxicity and their relative concentrations in EEE devices. As polymers, Acrylonitrile Butadiene Styrene (ABS), High Impact Polystyrene (HIPs), Polyamide (PA), and Polypropylene (PP) were selected given their significant use in EEE devices (w/w%), measured as polymer weight by device weight (Table 3). Other relevant polymers and additives for the EEE industrial sector were not included in this study due to limitations in time and data availability.

Table 4. Selected additives and polymers associated with the EEE industrial sector.

Additives	Flame retardants in e-waste			
	Brominated flame retardants (BFR)			
	PBDEs			
	pentaBDE	OctaBDE	DecaBDE	BTBPE

Polymers	Thermoplastic copolymer	Polystyrene	Polyolefins	Polyamide
	ABS	HIPS	PP	PA
	30%	25%	8%	3%

The physicochemical parameters additive molecular weight (MW), additive hydrophobicity (Kow), and polymer upper boundary diffusion value A*p (m2/s) and activation energies (τ, K) were gathered from different empirical experiments and databases. Kow and additive MW values were collected from ECHA, PubChem, and EPA databases. The author is aware of the use of plastic-water partitioning coefficients (Kpw) to estimate additive desorption rates from polymers and into water in previous studies (Allan et al., 2022; Sun et al., 2019). However, as Kpw data is not available for many polymer-additive pairs, this study worked based on additive octanol-water partitioning coefficient (Kow) assuming the octanol to be the organic phase in our polymer-water system. The complete input dataset can be found on the Supplementary Excel, worksheet Input dataset (complete).

Being aware of the limited available data on diffusion coefficient values for the selected additives, worst-case diffusion coefficients (D*p) were derived from Piringer Equation. Polymer-specific upper boundary diffusion value A'*p (m2/s) and activation energies (τ, K) were collected and adapted from (Plastics Europe, 2021) report. Given the absence of A'*p and τ values for ABS, input data for ABS was taken from SBS. This decision was made under the assumption that both copolymers, ABS and SBS, share a similar composition: Acrylonitrile Butadiene Styrene for ABS and Poly(styrene-butadiene-styrene) for SBS. The rationale behind this assumption is that the similarity in composition would translate into a similar structural conformation and, consequently, similar additive diffusion rates.

The complete input dataset can be found in the Supplementary Excel, worksheet *Input data (complete).*

PART 3. MODEL VALIDATION

Mathematical models are designed to mirror reality through the simplification of complex phenomena into mathematical equations, variables, and correlations. Yet, to demonstrate models' ability to accurately reflect and simulate the dynamics of the systems they represent, modeled predictions must be validated against empirical data. The process of validation of a mathematical model is understood as the operational validation (Tsioptsias et al., 2016).

Thereby, the operational validation process seeks to evaluate the accuracy and reliability of a model in simulating real-world outcomes. In the particular case of this study, the ARM's operational validation was performed by means of a proof of concept (i.e. first application of the model to estimate additive release) and the inclusion of a positive control.

3.1. Evaluation of PBDEs release estimations

Based on the ARM estimations of cumulative PBDEs mass (%) released at different temperatures and over time, a detailed inspection of additive release trends was performed. It aimed to prove the ARM's ability to qualitatively simulate additive release dynamics and the reproduction of additive release trends under different conditions and scenarios (i.e. additive release would decrease with polymeric size and increase with temperature) as shown in Figure 5.

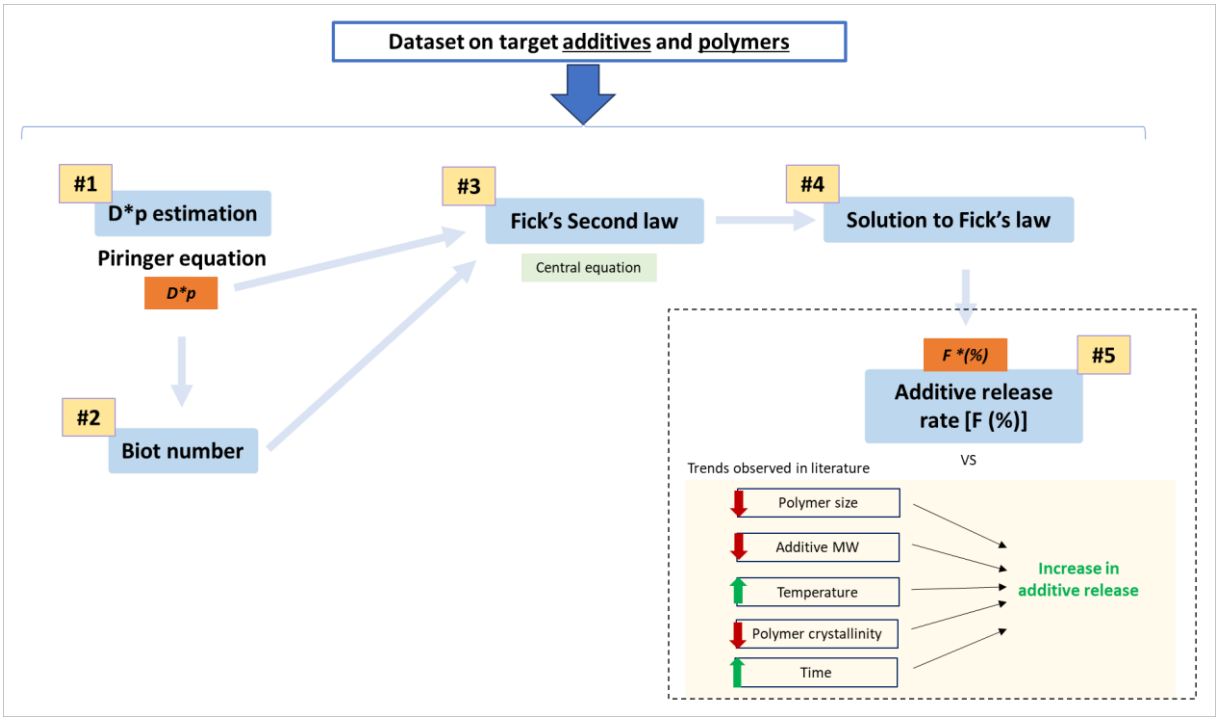

Figure 5. Simplified visualization of the qualitative control validation process. To prove the ability of the ARM to reproduce real-world additive release, the modeled %F estimations at varying conditions of time, temperature, polymer size, additive MW and polymer crystallinity were compared to additive release trends observed in the literature.

3.2. Positive control

The ARM's accuracy and reliability were likewise assessed by validating its output against specific empirical data (Figure 6). To that aim, the empirical study performed by Sun et al. (2019) was selected. Additionally, different sources were used to build a Diffusion Coefficient dataset based on empirical estimations.

Sun et al. (2019) studied the kinetics of decaBDE release from ABS plastic pellets (507µm sized) in sealed glass bottles using LDPE (Low-Density Polyethylene) films as an infinite sink over 150 days at 10°C and 30°C in aquatic conditions. Aiming to compare the measured data with the ARM output, the model conditions were set to mimic those adopted by Sun et al. (2019) (Table 5a). Next, the Diffusion Coefficient (Dp) values and Additive Release rate (F%) measured by Sun et al. (2019) (Table5b), were

compared to those estimated by the model. A general overview of the experiment conditions adopted from Sun et al. (2019) and entered into the model is displayed in Table 5.

Table 5. Experimental conditions and Dp and F (%) values collected from Sun et al. (2019). (a) Set of experimental conditions adopted from Sun et al. (2019) used to mimic the experimental setup. Aiming for simplification, the MNP size was approximated to 500 µm in the ARM. The original size was 507,5 µm. (b) Experimentally measured Dp and F(%) values obtained by Sun et al. (2019) under the conditions described in (a).

a

Environment	(Distilled) water
Temperature	30°C
Time (days)	0-150
Polymer	ABS
Polymer size (mean, µm)	500
Polymer radio (µm)	250
Additive(s)	BDE-209 (DecaBDE)

b

Dp (30°C)	$6.53E^{-26}$
F(%)	0.08

The ARM was run under the conditions described in Table 5a and using the estimated worst-case D*p value (D*p = $1.41E^{-15}$) for ABS, decaBDE, and at 30°C (Table 6, results). Seeking to prove the validity of the worst-case scenario estimation, the ARM was also run using the Dp value measured by Sun et al. (2019) (Table 5b, Dp = $6.53E^{-26}$). This second estimation was introduced as a positive control for the Piringer Equation (Eq. 3).

In parallel, a batch of experimentally determined diffusion coefficient values (Dp) was collected from the literature (Sup. Excel, worksheet *Input data (complete)*). Empirical Dp values for decaBDE and BTBPE in ABS polymers were collected from Sun et al. (2019). To complete our dataset, the average Dp estimation from the 10 PBDE examined in the same study (BDE-7, BDE-15, BDE-118, BDE-138, BDE-153, BDE-206, BDE-207, BDE-208, BDE-209, BTBPE) at 30°C was used for pentaBDE and octaBDE. Dp (20°C) values for the polymer PA were collected from Sun et al. (2019). PA values were obtained using a linear correlation between PBDEs diffusion in different polymers and the glass transition temperature (Tg). Finally, the empirical Dp values for PP (at 25°C) represent the averaged estimates of Dp values for PBDEs within PP polymer, as demonstrated by Allan et al. (2022). Notice that Dp values for HIPS were not found in the literature and, therefore, are not presented. Next, collected Dp values were compared to our D*p estimations.

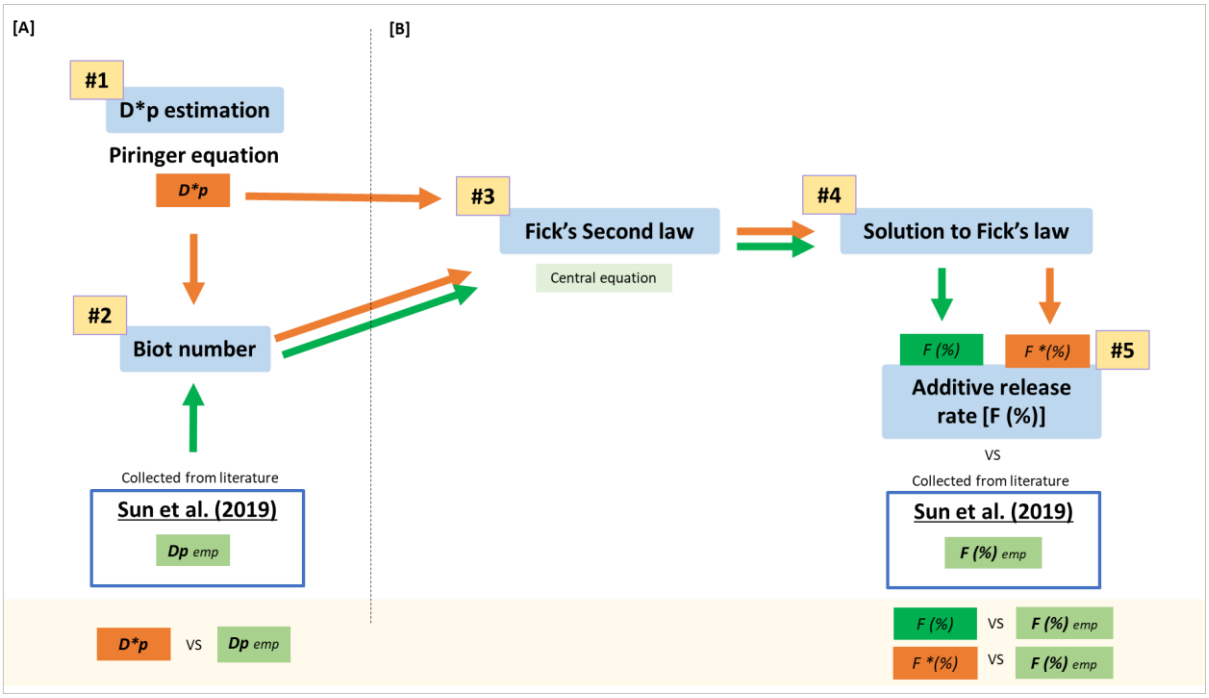

Figure 6. Simplified visualization of the positive control validation process. (A) Worst-case scenario diffusion coefficient values (D*p) were modeled for decaBDE and ABS polymer at 30°C with Piringer Equation. Next, D*p and the empirically measured Dp were compared. (B) Orange arrows represent the steps followed to model the worst-case additive release rate (F*%) based on Piringer's diffusion coefficient (D*p). Green arrows represent the steps followed to model the additive release rate based on the diffusion coefficient measured by Sun et al. (2019), Dp. Dp_{emp} and $F(\%)_{emp}$ indicate the empirical values estimated in the literature.

RESULTS

The release of pentaBDE, octaBDE, decaBDE, and BTBPE from the polymers ABS, HIPS, PP, and PA was modeled under varying conditions of time and temperature. To validate the model operationally, the resulting additive release trends were assessed as functions of time (t), temperature (T), polymer type, and additive molecular weight (MW). Simultaneously, a positive control was introduced to demonstrate the accuracy and reliability of the model output through validation against empirical data. A complete overview of the ARM's estimations and the detailed model calculations can be found in the Supplementary Excel.

1. Worst-case scenario Diffusion Coefficients

D*p is a polymer-specific upper-bound diffusion coefficient. It represents the highest rate (i.e. *worst-case scenario)* at which additives diffuse within a polymeric matrix under specific conditions of temperature (T), additive MW, and polymer type.

As shown in Table 6, D*p values varied with temperature, additive MW, and polymer type. Despite the marked consistency in diffusion coefficients displayed for each polymer, significant differences are observed between groups, suggesting the clear influence of polymer type on additive diffusivity (i.e. 3.2 E-17 – 6.2 E-14 for ABS; 8.8E-22 – 1.7E-18 for HIPS; 1.34E-18 – 5.42E-15 for PP; and 1.71E-20 – 1.26E-17 for PA). Overall, additive diffusion coefficients increased with temperature. At 40°C, the highest values for D*p were observed for every additive in the four different polymers. The

results also evidence the strong influence of additive MW (g/mol) on additive diffusivity with the highest D*p values reported for pentaBDE (564.69 g/mol). the additive with the lower molecular weight, followed by BTBPE (687.6 g/mol), octaBDE (801.47 g/mol), and decaBDE (952.22 g/mol). A*p estimations and input data can be found in Annex 3.

Table 6. Summary of worst-case scenario Diffusion Coefficients (D*p) estimated with Piringer Equation (Eq. 3) for the four selected additives (pentaBDE (564.69 g/mol); octaBDE (801.47 g/mol); decaBDE (952.22 g/mol); BTBPE (687.6 g/mol)) per polymer (ABS, HIPS, PP and PA) at varying temperatures (°C). D*p values are estimated as a function of polymer type, additive MW, and temperature (T). D*p values are polymer size- and time-independent.

	D*p (m2 s-1)				
	ABS				
Additives	0°C	10°C	25°C	30°C	40°C
pentaBDE	4.67E-16	1.80E-15	1.16E-14	2.06E-14	6.20E-14
OctaBDE	8.40E-17	3.25E-16	2.08E-15	3.71E-15	1.12E-14
DecaBDE	3.20E-17	1.24E-16	7.91E-16	1.41E-15	4.24E-15
BTBPE	1.85E-16	7.15E-16	4.58E-15	8.17E-15	2,46E-14

	D*p (m2 s-1)				
	HIPS				
Additives	0°C	10°C	25°C	30°C	40°C
pentaBDE	1.28E-20	4.95E-20	3.17E-19	5.65E-19	1.70E-18
OctaBDE	2.30E-21	8.90E-21	5.71E-20	1.02E-19	3.06E-19
DecaBDE	8.77E-22	3.39E-21	2.17E-20	3.87E-20	1.17E-19
BTBPE	5.08E-21	1.96E-20	1.26E-19	2.24E-19	6.74E-19

	D*p (m2 s-1)				
	PP				
Additives	0°C	10°C	25°C	30°C	40°C
pentaBDE	1.95E-17	9.25E-17	7.85E-16	1.53E-15	5.42E-15
OctaBDE	3.52E-18	1.67E-17	1.41E-16	2.75E-16	9.76E-16
DecaBDE	1.34E-18	6.34E-18	5.38E-17	1.05E-16	3.71E-16
BTBPE	7.74E-18	3.67E-17	3.11E-16	5.55E-16	2.15E-15

	D*p (m2 s-1)				
	PA				
Additives	0°C	10°C	25°C	30°C	40°C
pentaBDE	9.49E-20	3.67E-19	2.35E-18	4.19E-18	1.26E-17
OctaBDE	1.71E-20	6.60E-20	4.23E-19	7.54E-19	2.27E-18
DecaBDE	6.50E-21	2.51E-20	1.61E-19	2.87E-19	8.64E-19
BTBPE	3.76E-20	1.45E-19	9.32E-19	1.66E-18	5.00E-18

2. Rate limiting steps for additive release

Bi was calculated as a function of additive diffusivity in water (Dw), additive diffusivity within the polymer (Dp), additive octanol-water partitioning coefficient (Kow), polymer size (Lc), and water presence in the surrounding environment (δw). Resulting Bi estimations for MNPs sized 1 µm and 500 µm at varying temperatures are displayed in Table 7 for the target additives. The four polymers under study were considered. If Bi>1, additive release abides by Case I, in which additive diffusion through the polymeric matrix is the rate-limiting step. Case II occurs when the Bi value hovers around 1, meaning the rate of both diffusion steps is almost equal. If Bi <1, additive external diffusion is slower, being that the limiting step and Case III would apply.

Overall, MNPs (500 µm) exhibited higher Bi values compared to MNPs sized 1 µm, evidencing the marked influence of polymer size on establishing the controlling step in additive diffusivity. While for MNPs sized 500 µm Bi values ranged from 0.083 - 144.6 for ABS; 3033.03– 5273988.65 for HIPS; 0.95– 3456.5 for PP; and 409.16 – 711148.46 for PA. For both sizes, large relative variations in Bi values within polymer types (ABS, HIPS, PP, PA) were observed as a function of additive type and temperature. As common trends, Bi values decreased with increasing temperature and decaBDE showed the highest relative Bi value, evidencing the indirect influence of temperature and the direct effect of additive MW on Bi estimations, respectively. Yet, a marked consistency was observed upon assignation of the rate-limiting step to each of the polymeric groups.

For 1 µm MNPs, PA and HIPs exhibited Bi>1 at any given temperature and additive species, exhibiting the highest values for 1 µm MNPs at the lowest temperatures considered (Table 7A). For ABS, Bi values suggested a slower external diffusion (Bi>1) at every temperature except for the larger additives (octaBDE and decaBDE) at 0°C, which displayed a Bi close to 1. An externally controlled diffusion (Bi>1) was likewise observed for every additive in PP polymers at 25°C (except for decaBDE), 30°C, and 40°C. However, at 0°C, diffusion in PP was internally controlled (Bi>1) for octaBDE and decaBDE while Bi=1 was observed for pentaBDe and BTBP. For MNPs sized 500 µm, resulting Bi values were in every case above 1, indicating that additive release is internally controlled (Case I). The same trends as those were described for 1 µm MNPs as a function of temperature, additive MW, and polymer type apply (Table 7B).

Solution to Case II (Bi =1)

Case II occurs when the Bi value hovers around 1 (values highlighted in green in Table 7), meaning the rate of both diffusion steps is almost equal. Under this scenario, a careful screening of the ongoing tendency should be performed to apply the most accurate solution to Fick's law. To substitute Bi=1 values, ABS polymer 500 µm size was used as the proof of concept.

As observed in Table 18 (Annex 5), when assuming internally-controlled diffusion (Bi>1, Case I) for those additives showing Bi=1 (Case II, highlighted in green, Table 7), a gradual increase in cumulative additive mass (%) released from polymers was observed as a function of time and temperature. In contrast, if assuming externally-controlled diffusivity (Bi<1, Case III) for those cases with Bi=1 (Case II), the model predicted no additive release from the polymer at the highest temperatures and the effect of time would be negligible. Such Thereby, when applying Case I (Bi>1) to substitute for Bi=1, observed trends on additive release were in line with the described effect of temperature and time in the literature. In contrast, the application of Bi<1 (Case III), contradicts the additive release patterns reported in existing studies (Table 2). Thereby, further research needs to be done to shed light on the validity of the solution to Case III. Yet, given the accuracy of Case I solution to 'ick's second law to reproduce additive release patterns at varying conditions and over time, Bi >1 was applied to estimate the released additive mass fraction [1 – F(%)] in this study when Bi=1 for MNPs sized 1 µm and 500 µm.

Table 7. Summary of Bi values calculated for at varying temperatures (0, 10, 25, 30, 40°C) based on the worst case scenario D*p values (Table 6). (A) Bi values for MNPs sized 1µm. (B) Bi values for MNPs sized 500µm. Bi > 0.1 values (highlighted in blue) indicate that internal diffusion (Step 1) is the rate-limiting step. Bi < 0.1 values (highlighted in orange) indicate that external diffusion (Step 2) is the rate-limiting step.

A	Bi (0°C)	Bi (10°C)	Bi (25°C)	Bi (30°C)	Bi (40°C)
ABS (SBS)					
pentaBDE	0.022	0.006	0.001	0.000	0.000
OctaBDE	0.116	0.030	0.005	0.003	0.001
DecaBDE	0.285	0.074	0.012	0.006	0.002
BTBPE	0.037	0.010	0.002	0.001	0.000
HIPS					
pentaBDE	793.885	205.441	32.057	17.978	5.976
OctaBDE	4222.389	1092.666	170.498	95.618	31.786
DecaBDE	10392.096	2689.256	419.629	235.334	78.232
BTBPE	1354.870	350.612	54.709	30.682	10.200
PP					
pentaBDE	0.520	0.110	0.013	0.007	0.002
OctaBDE	2.767	0.584	0.069	0.035	0.010
DecaBDE	6.811	1.438	0.170	0.087	0.025
BTBPE	0.888	0.187	0.022	0.012	0.003
PA					
pentaBDE	107.048	27.705	4.324	2.425	0.806
OctaBDE	569.350	147.355	22.997	12.898	4.288
DecaBDE	1401.278	362.668	56.600	31.744	10.554
BTBPE	182.69	47.28	7.38	4.14	1.38

B	Bi (0°C)	Bi (10°C)	Bi (25°C)	Bi (30°C)	Bi (40°C)
ABS (SBS)					
pentaBDE	11.054	2.861	0.446	0.250	0.083
OctaBDE	58.791	15.216	2.375	1.332	0.443
DecaBDE	144.696	37.449	5.845	3.278	1.090
BTBPE	18.865	4.882	0.762	0.427	0.142
HIPS					
pentaBDE	402896.887	104261.263	16268.810	9123.790	3033.035
OctaBDE	2142862.213	554527.788	86527.892	48526.123	16131.614
DecaBDE	5273988.654	1364797.627	212961.486	119431.955	39702.949
BTBPE	687596.451	177935.537	27764.861	15570.945	5176.273
PP					
pentaBDE	264.056	55.735	6.573	3.378	0.951
OctaBDE	1404.416	296.435	34.958	17.968	5.060
DecaBDE	3456.532	729.582	86.039	44.223	12.452
BTBPE	450.645	95.119	11.217	6.291	1.623
PA					
pentaBDE	54326.909	14060.482	2194.372	1230.704	409.168
OctaBDE	288945.100	74782.599	11671.066	6545.669	2176.216
DecaBDE	711148.468	184054.101	28724.698	16110.127	5356.079
BTBPE	92716.006	23996.060	3744.984	2100.358	698.299

3. Released fractions of PBDEs

Using the ARM's estimations of cumulative PBDEs mass (%) released across various temperatures and durations, a thorough examination of additive release patterns was conducted. The objective was to demonstrate the ARM's capability to simulate the dynamics of additive release and accurately replicate additive release trends across diverse conditions and scenarios (i.e. at varying conditions of time (t), temperature (T), additive MW and polymer type). The complete dataset on released additive mass fraction [1 – F (%)] can be found in Annex 6 and Annex 7 or in the Sup. Excel, worksheets *F% 1µm* and *F% 500µm*, respectively.

Effect of size

As depicted in Figure 7, additive release was influenced by polymer size, with relatively higher loss rate for smaller polymers. While the cumulative mass fraction released was of 100% at any timepoint for 1 µm, MNPs sized 500 µm exhibited a gradual increase in additive loss, with a release of 14.2% on day 1 and reaching the 99,9% additive loss after one year. The reference dataset is displayed in Sup. Excel, worksheet *Trends*.

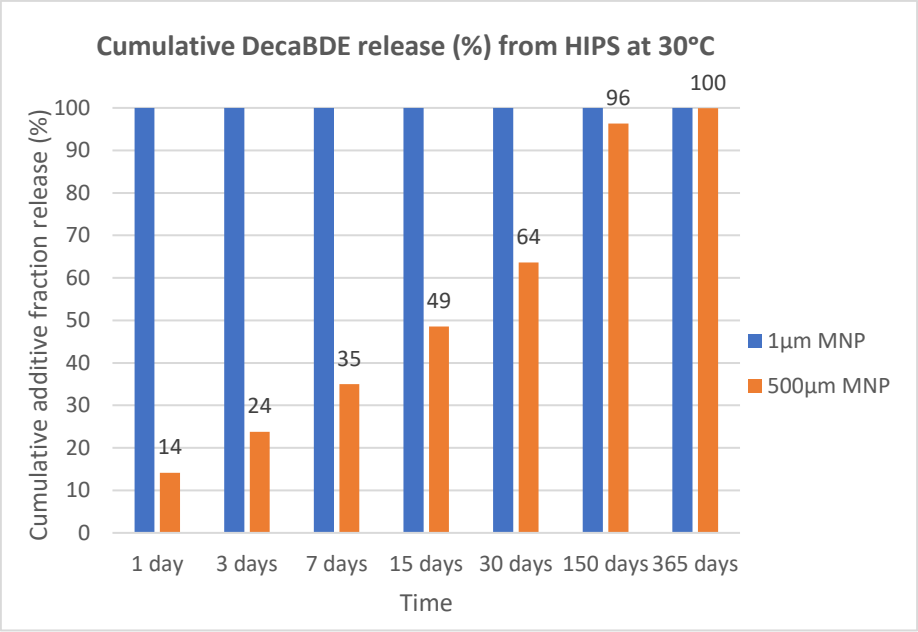

Figure 7. Cumulative mass of decaBDE released at 30°C from HIPS 1 µm and 500 µm as a function of MNP size.

Effect of temperature

The effect of temperature was inspected upon comparison of the cumulative release of decaBDE from PP at varying temperatures. As depicted in Figure 8, the complete release of decaBDE was observed after 150 days at 40°C, and after 365 days at 25°C at 30°C. A more gradual response and lower released mass fractions after 356 days were obtained at 10°C at 0°C, with the estimated loss of 58.47% and 30.24% of decaBDE, respectively. The reference dataset is displayed in Sup. Excel, worksheet *Trends*.

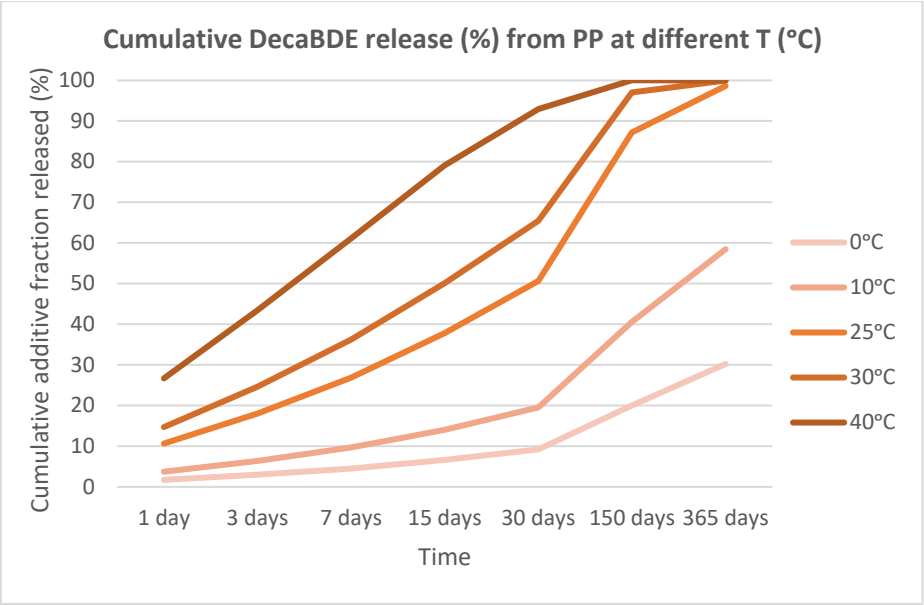

Figure 8. Cumulative mass of decaBDE released from PP at varying temperatures (°C) as a function of temperature.

Effect of additive MW

The additive release trends observed in Figure 9 evidence the strong influence of additive MW (g/mol) on additive diffusivity with the faster additive release reported for pentaBDE (564.69 g/mol), the additive with the lower molecular weight, followed by BTBPE (687.6 g/mol), octaBDE (801.47 g/mol), and decaBDE (952.2 g/mol). The reference dataset is displayed in Sup. Excel, worksheet *Trends*.

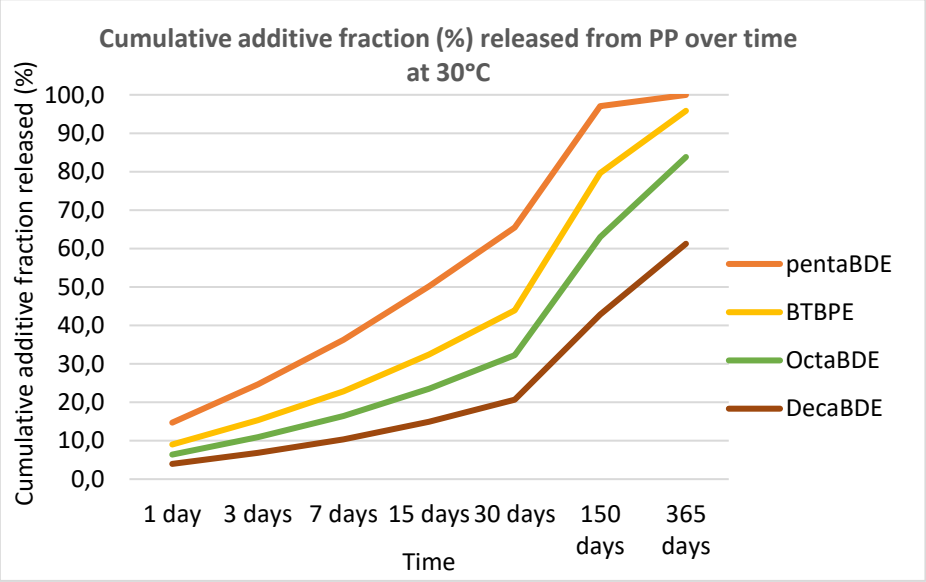

Figure 9. Cumulative additive fraction (%) released from PP over time at 30°C as a function of additive MW. The graph shows the cumulative additive release of pentaBDE (564.69 g/mol), BTBPE (687.6 g/mol), octaBDE (801.7 g/mol), and decaBDE (952.22 g/mol).

Effect of polymer type and additive MW

The ARM output showed the marked influence of polymer type on additive release. As depicted in Figure 10, cumulative additive release from HIPS and PA ranged 19.01% - 61.28% and 46.83% - 98.58%, respectively, exhibiting a relatively lower loss of additives when compared to the estimations reported for PP (100%) and ABS (100%). As observed in Table X, the smallest additive (pentaBDE) showed the highest additive release rate, followed by BTBPE, octaBDE, and decaBDE. The reference dataset is displayed in Sup. Excel, worksheet *Trends*.

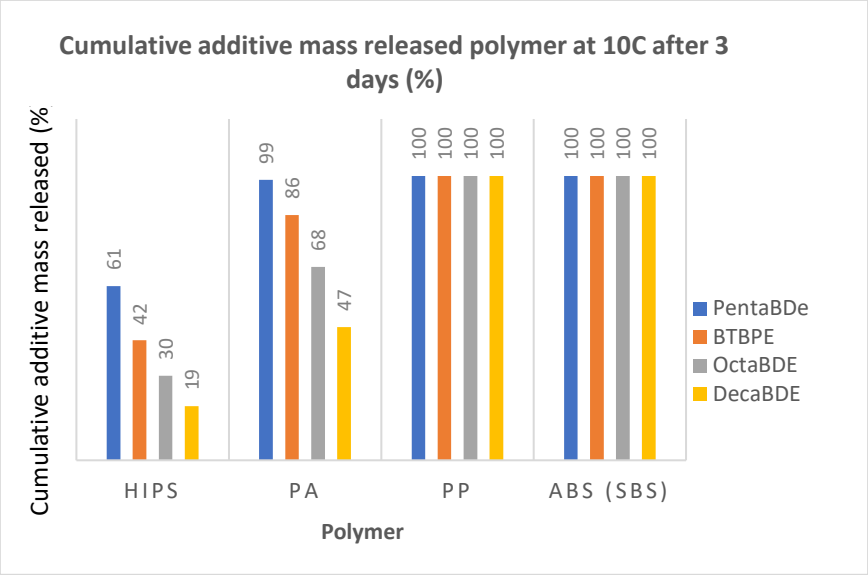

Figure 10. Cumulative additive mass released polymer at 10°C after 3 days (%) as a function of polymer type.

4. Positive control

The accuracy and reliability of the ARM were evaluated by comparing its output with empirical data. To that aim, the experiment conducted by Sun et al. (2019) was selected as the positive control of reference.

Sun et al. (2019) investigated the release kinetics of decaBDE from ABS plastic pellets of 507µm size placed in sealed glass bottles with LDPE films as an infinite sink in an aquatic media. The experiment lasted 150 days and was conducted at 10°C and 30°C. Our ARM was run under the same conditions and the output was compared against the Dp and F (%) values obtained by Sun et al. (2019). For the sake of simplicity, ABS was assumed to be 500 µm size in our model.

Beyond Sun et al. (2019), additional sources were used to build a more complete empirical Diffusion Coefficient dataset for Piringer's Equation validation.

Estimation of worst-case scenario Diffusion Coefficients (D*p)

In our ARM, the Piringer Equation estimates the worst-case scenario for additive diffusivity. Thereby, D*p values were expected always to be slightly higher than those measured experimentally

(D*p > Dp). Only D*p estimations for PP comply with our hypothesis, with 7.8E-16 (D*p) > 3.2E-17 (Dp) for pentaBDE; 1.4E-16 (D*p) > 3.2E-17 (Dp) for octaBDE; and 5.4E-17 (D*p) > 3.2E-17 (Dp) for decaBDE (Table 8B).

In contrast, for ABS (Table 8A) and PA (Table 8C), worst-case scenario D*p values were in every case significantly higher (closer to 0) compared to Dp estimations. For instance, experimentally measured decaBDE diffusivity in ABS was 6.5E-26 while the D*p estimation was various orders of magnitude higher, 1,4E-15. A similar disparity was observed for pentaBDE (D*p, 2.1E-14; Dp, 7.0E-24), octaBDE (D*p, 2.1E-14; Dp, 7.0E-24), and BTBPE (D*p, 8.2E-15; Dp, 1.1E-24) in ABS polymers. Following a similar pattern, an evident contrast between modeled and empirically measured diffusion coefficients was likewise observed for PA, with D*p values ranging from 2,35E-18 to 1,61E-19 and Dp ranging from 4,86E-23 to 1,15E-25.

Table 8. Comparison of Diffusion Coefficient values empirically measured (Dp emp) and calculated with the ARM (D*p) for the selected additives in ABS polymer at 30°C and PP polymer at 25°C. Empirical Dp values for ABS were reported by Sun et al. (2019). Dp values for pentaBDe and octaPBE were estimated as an average of the Dp values from the entire set of PBDEs under study by Sun et al. (2019). Estimations on Dp (20*C) values for PA were obtained using the linear correlation between PBDEs diffusion in different polymers and the glass transition temperature in the same study. Empirical Dp values for PP (25°C) were collected from John Allan et al. (2022).

	A		B		C	
	ABS (30°C)		**PP (25°C)**		**PA (25°C & 20°C)**	
	Model	Literature	Model	Literature	Model	Literature
Additives	**D*p**	**Dp**	**D*p**	**Dp**	**D*p (25°C)**	**Dp (20°C)**
pentaBDE	2.1E-14	7.0E-24	7.8E-16	3.2E-17	2.35E-18	4.86E-23
OctaBDE	3.7E-15	7.0E-24	1.4E-16	3.2E-17	4.23E-19	4.86E-23
DecaBDE	1.4E-15	6.5E-26	5.4E-17	3.2E-17	1.61E-19	1.15E-25
BTBPE	8.2E-15	1.1E-24	-	-	-	-

Biot number

The Biot number was calculated to determine whether internal or external diffusion was the rate-limiting step in the mass transport diffusivity of decaBDE within 500 µm-sized ABS particles.

The Biot number is dependent on the additive diffusivity rate (Dp). Therefore, due to the discrepancies observed between Dp and D*p estimations presented in Table 8A, the Biot number (Bi) was computed twice: once using Dp values and once using D*p values. As illustrated in Table 9 below, both Bi values suggested internally-controlled additive diffusivity regardless of the diffusion coefficient used in the estimation; however, Bi values based on empirical Dp estimations were notably higher.

Table 9. Comparison of Bi values calculated for MNPs 500µm sized. Modeled Bi values were computed based on D*p estimations for decaBDE in ABS at 30°C from this study. Literature Bi values were estimated with Dp from Sun et al. (2019) for decaBDE in ABS at 30°C.

	Based on D*p, model	**Based on Dp, Sun et al., (2019)**
Diffusion coefficient	1.4E-15	6.5E-26
Biot number	3.28	70820161170.27

Release of decaBDE from ABS (500 µm) at 30°C over 150 days

Additive release (i.e. [100-F(%)]) was modeled under two scenarios. First, the ARM was run considering the empirical diffusion coefficient provided by Sun et al. (2019), Dp. Next, the ARM estimations were based on D*p values. As shown in Table 10, a marked mismatching between ARM's release estimations was obtained.

Additive release estimations based on D*p, showed the almost complete decaBDE release (96.3%). In contrast, the ARM estimations based on Dp values (Sun et al., 2019) indicated that only of 0.012% decaBDE would be released under the same conditions. The former value was relatively high when contrasted with the released decaBDE fraction reported by Sun et al. (2019) for plastic A and plastic B, 0.115% and 0.038%, respectively.

Table 10. Summary of estimations on the additive mass fraction (F%) released from ABS polymers based on different Diffusion coefficient values. The ARM estimations were made twice, based on the worst-case scenario diffusion coefficient (D*p) estimated in this study with the ARM (a) and on the empirically measured diffusion coefficient (Dp) by Sun et al., 2019 (b).

	Model		Literature	
	ARM + D*p	ARM + Dp	Sun et al., (2019)	
			Plastic A (ABS)	Plastic B (ABS)
Diffusion Coefficient 30°C	D*p (a)	Dp (b)	Dp (b)	Dp (b)
	1.41E-15	6.53E-26	6.53E-26	6.53E-26
F (%)	0.0369	0.9999	-	-
[1 – F (%)]	0.9631	0.0001	0.0011	0.0004
[1 – F (%)] * 100	96.3148	0.0121	0.1149	0.0384

a. Worst-case scenario diffusion coefficient (D*p) estimated in this study with the ARM
b. Empirically measured diffusion coefficient (Dp) by Sun et al., 2019.

5. Model validation

Qualitative and quantitative operational validation are two approaches used to assess a mathematical model's accuracy, reliability, and effectiveness in representing real-world systems.

Qualitative operational validation involves assessing the model's performance based on its ability to capture the system's behaviors being modeled. Here, the validity of the ARM was determined qualitatively by assessing its ability to replicate real-world trends in additive release under varying conditions of time, temperature, polymer size and type, and additive MW. Such trends are presented in Table 2. In this study, the qualitative validity of the model was assessed in light of previous literature.

The quantitative operational validation of a model relies on quantitative comparisons between the model's outputs and empirical data collected from the real-world system (i.e. positive controls). It aims to evaluate its accuracy and reliability in predicting the system's outcome. This study used empirical Dp estimations to prove the validity of Piringer's Equation. Additionally, the estimations on additive release measured by Sun et al. (2019) were used as a positive control.

Piringer equation appears to be a reliable tool for estimating D*p

Given that the Piringer equation (Eq. 3) estimates the worst-case scenario, D*p values were expected to be similar to or slightly higher than those reported in empirical studies (D*p ≥ Dp).

However, as summarized in Table 8, D*p estimations for PA and ABS proved not to reproduce literature data, with D*p values several orders of magnitude higher (i.e. pentaBDE, 2.1E-14 (D*p), 7.0E-21 (Dp)). Under these observations, we hypothesized that potential errors in the modeling process could have occurred. These errors could stem from either 1) issues with the mathematical methodology or 2) inaccuracies within the input data.

In contrast, D*p estimations for PP were in agreement with our hypothesis (D*p ≥ Dp) suggesting the Piringer Equation's effective performance. Additionally, previous studies using the Piringer equation such as the one performed have reported reliable estimations of D*p values when compared to literature Dp (Begley et al., 2005; Nguyen et al., 2013b; Plastics Europe, 2021). Consequently, Piringer's Equation was assumed to be a reliable approximation for reproducing the ARM's worst-case scenario additive diffusivity in the ARM. Hence, focus was put on the input dataset to explain the notable disparity between Dp and D*p values.

The inaccuracy of the input dataset did not affect ARM's qualitative performance

The inaccuracy of D*p estimations (Table 8) was reflected in discrepancies in the [100-F(%)] output. Assuming the validity of the Piringer Equation, a thorough screening of the input dataset was conducted.

Inaccuracies in polymer-related parameters were found for ABS, PA, and HIPS. Collected A'*p (m2/s) values for PA, ABS, and HIPS appeared to be only applicable to estimate the diffusivity of additives with smaller molecular size (MW) than those selected in this study (Table 11). This observation may underpin the obtained mismatch between literature Dp and D*p estimations for PA and ABS, suggesting that a higher degree of overestimation (%) should be added to the ARM output.

Table 11. (A) Additive MW range used in A*'p estimations. A*'p were then collected from source Plastics Europe 2021 and used as input data for this model. (B) Summary of target additives in this study and their additive molecular weight (MW).

A	
Polymer	Additive MW (g/mol)
HIPS	104-430
PA	32-587
PP	30-2000
ABS (SBS*)	84-689

B	
Additive	MW (g/mol)
pentaBDE	564.69
OctaBDE	801.47
DecaBDE	952.22
BTBPE	687.6

However, the difference between Dp-D*p for ABS seemed notably greater than the reported difference for PA and HIPS. Given the absence of A'*p and τ (K) values for ABS, input data for ABS was taken from SBS. This decision was made assuming that both copolymers, ABS and SBS, share a similar composition: Acrylonitrile Butadiene Styrene for ABS and Poly(styrene-butadiene-styrene) for SBS. The rationale behind this assumption is that the structural conformation of both polymers would be similar. However, differences in the parameter glass transition temperature (Tg) was overlooked. Tg values must be considered to associate polymer type with additive diffusivity and, consequently, with additive release rates (Allan et al., 2022; Sun et al., 2019). The parameter glass transition temperature (Tg) reflects the structural conformation of the polymeric chains in the plastic matrix, which ranges between crystalline and amorphous. More amorphous polymers present random chemical dispositions, spaces

between polymeric chains, and low glass transition temperatures (Tg), resulting in higher additive diffusivity rates (Allan et al., 2022; Askadskii et al., 2014; Petrovics et al., 2023; Sun et al., 2019)

As shown in Table 12, the Tg values of both types of plastic were markedly different. In ABS, acrylonitrile is the main monomer type in the copolymer. It provides a solid primary structure to the material (Izdebska & Thomas, 2016). The absence of the monomer acrylonitrile in SBS results in a more flexible and significantly more amorphous type of polymer. Such structural difference is hypothesized to translate into lower Tg and higher additive diffusivity (i.e. lower D*p values) for SBS, as evidenced in Table 12 (Cao et al., 2023). Thereby, the SBS input dataset was not applicable to estimate additive release from ABS polymer. Consequently, the inclusion of ABS as a target polymer was eventually disregarded. The output data from the ARM was assessed with SBS as the target polymer.

Table 12. Summary of the glass transition temperature values for the target polymers. Minimum (Tg min) and maximum (Tg max) glass transition values are displayed. SBS copolymer is composed of two polymeric segments, a more crystalline section of Polystyrene (PS, Tg=70°C) and Polybutadiene (PB, Tg=-80°C) (Cao 2023).

Polymer	Tg min	Tg max
ABS	90	102
HIPS	88	92
PA	35	45
PP	-20	-10
SBS	-80	70

In this context, the ARM output was addressed under two premises during the qualitative validation of the model. First, due to disparities in additive molecular weights, an additional level of overestimation was assumed for the release rates of SBS, HIPS, and PA. Secondly, the use of ABS as a target polymer was dismissed despite its high weight percentage (w/w%) in EEE devices. SBS was considered instead.

The ARM reproduces qualitative additive release behavior under Case I scenario (Bi >1)

The ARM developed in this study was found to be a reliable tool to reproduce additive release trends under Case I. Case I occurs under internally controlled diffusivity, meaning additive diffusion within the polymeric matrix acts as the rate-limiting step (Figure 1). In the ARM, this internally controlled diffusivity applies when Bi >1.

The ARM output revealed cumulative additive release mass over time and as a function of temperature (Figure 8) These results are consistent with additive loss kinetics described in previous studies. For instance, the progressive loss of BFRs from two ABS microplastic pellets at 10°C and 30°C during a time-course of 150 days was reported by Sun et al. (2019). Likewise, Paluselli et al. (2019) observed the cumulative loss of additives dimethyl phthalate (DMP) and diethyl phthalate (DEP) from PVC-cables over a 90 days laboratory experiment. This positive correlation between additive loss, increasing temperatures, and time was also evidenced by Dimassi et al. (2023) upon estimation of additive leaching of bis(2-ethylhexyl) phthalate (DEHP) under extreme simulated marine conditions over 140 days.

Beyond time and temperature, additive molecular weight also played a role in additive release kinetics (Figure 9). Regardless of the type of polymer, the highest additive release rates were reported for pentaBDE, the smallest polymer (564.69 g/mol), followed by BTBPE (687.6 g/mol), octaBDE (801.47

g/mol) and decaBDE (952.22 g/mol). These observations aligned with our hypothesis and previous observations (Dong & Gijsman, 2010; Fauvelle et al., 2021; Paluselli et al., 2019; Teuten et al., 2009; Zhou et al., 2017). For instance, Paluselli et al. (2019) observed selected migration resulting from differences in additive MW between the seven phthalic acid esters (PAEs) under study (i.e. DMP, DEP, DPP, DiBP, DnBP, BzBP, DEHP) from PVC-cables and PE-bags. In PVC-cables, additive release was only reported for the low-molecular-weight additives DMP and DEP. In contrast, bigger-MW additives such as DEHP did not release out of the polymer. Under these observations, it was assumed that the higher size, hydrophobicity, and thereby higher Kow, would have hampered the migration and release of DEHP during the assessed time-course.

The effect of polymer size is evidenced by our results. Overall, higher additive release rates were observed for the small MNP size considered (1 µm). This size effect stems from the large surface area of the smallest MNPs in relation to the overall mass, allowing for higher additive desorption rates from on the MNPs' surface. This, in turn, may enhance the internal negative concentration range (Dong & Gijsman, 2010; Zhou et al., 2017). Interestingly, we observed the complete loss of 100% additive content for 1 µm SBS and PP MNPs, the more amorphous and flexible polymers, even on day 1 and at 0°C (Annex 7; ABS). A similar effect was reported by Paluselli et al. (2019) in aquatic conditions. Compared to the release from the thicker and structurally consistent PVC-cables, no release of the low-weight additives was detected from the thinner and more flexible PE-bags, suggesting their complete release even before the experiment due to PE-bag larger surface area.

Finally, a marked difference in additive release rates was observed between polymers regardless of MNPs size. The polymer type factor is included in the model in Piringer Equation with the upper-boundary diffusion coefficient (A*p). Thereby, differences in polymer type were expected to define additive diffusion rates (D*p) and, ultimately, additive release estimations. Higher D*p values (i.e. closer to 0) result in reduced additive diffusivity and lower release rates.

In this study, the highest additive release rates [100-(F%)] were obtained for the SBS polymer for both considered sizes, 1µm (Annex 6) and 500µm MNPs (Annex 7), and every type of additive (i.e. pentaBDE, octaBDE, decaBDE, BTBPE). Compared to SBS, PP displayed slightly lower additive release rates, followed by the polymer PA. Finally, the polymer HIPS displayed the lowest additive release estimations. According to the literature, high Tg values result in increased additive diffusivity (Dp) and lower release rate (Rusina et al., 2007, 2010). In line with this statement, the highest D*p estimations and release rates belonged to the polymer with higher Tg, HIPS (Table 12), followed by PA, PP, and SBS. Combined, these observations suggest the ARM accuracy to represent the strong correlation between polymer structure, additive diffusivity, and additive release rate.

Thereby, the obtained ARM output under B >1 suggested the accuracy of the model at the qualitative operational level. That is, the model reproduces real-world additive release behavior under varying conditions of time, temperature, and size for the different additives and polymers considered according to the patterns displayed in Table 2.

The ARM solution under Case III (Bi<1) does not reflect additive release behavior

Additive diffusivity appeared as externally controlled (Bi<1) only for ABS and PP sized 1µm. Under Bi<1, internal diffusion outpaces external desorption and diffusion in the aqueous phase (Table 7). This scenario was expected for ABS and PP given their low Tg values (Table 12) and relatively small D*p values (Table 6). Additionally, the smallest Bi estimations were obtained at higher temperatures (25°C, 30°C, 40°C) and for pentaBDE and BTBPE, the low-weight additives. These results suggested that the

reduced polymer size enhanced the internal diffusion rate of the smallest additives at relatively high temperatures.

However, contrary to our expectations, the application of Case III solution to Fick's law for ABS and PP sized 1µm resulted in a released mass fraction of 0% in all cases (Table 17, Annex 4). This contrasted with the higher releases observed for ABS and PP sized 500 µm. For instance, 40.76% and 26.98% of pentaBE and BTBPE were estimated to be released after 30 days at 0 °C from ABS, respectively. Considering the effect of size, we expected higher release rates for MNPs sized 1µm. Combined, these observations suggest a lack of accuracy on Fick's law solution under Bi<1 with the ARM not reproducing the hypothesized additive release trends.

DISCUSSION

1. The ARM's scope of applicability

The estimations on decaBDE release from ABS modeled by the ARM when using empirical Dp estimations are in good agreement with those reported by Sun et al. (2019). Additionally, additive release trends under varying conditions complied with those trends described in the literature when internal diffusivity was the rate-limiting step. Combined, these observations suggest that the ARM can reliably estimate internally-controlled additive release based on empirical Dp values.

Nonetheless, it should be underlined that the ARM does not consider crucial physicochemical processes undergone by additives upon release into the environments. Upon release, additives may biodegrade or transform into secondary products, be transported to other compartments, sorpt onto organic matter or accumulate in organisms (Van Den Berg et al., 1995; T. Wang et al., 2023). Consequently, the initial release concentration may evolve over time and under specific environmental conditions, increasing or diminishing the effective environmental exposure. Hence, when interpreting the ARM estimations, it is essential to consider that this first ARM version overlooks the relevance of these physicochemical processes**.** To address this gap, data regarding additive transformation, transport, and fate must always be used to inform possible over or underestimations. Future efforts should focus on including the processes of additive persistence, transport, and fate into the ARM for a more complete exposure assessment.

On the same note, it is important to mention that the ARM is designed to run per environmental compartment. Given that environmental compartments are not entirely isolated, additives are expected to diffuse within and between them, causing the initially released concentrations to gradually diminish. Nevertheless, since plastic loss into the environment follows a systematic and consistent pattern, particularly at accumulation hotspots, the ARM can provide insights into the rates of additive release in those areas.

2. Addressing the knowledge gap

Existing plastic Environmental Risk Assessment (ERA) studies do not consider additive loss despite the growing body of evidence that, over the last decades, has shed light on the toxicity of plastic additives upon release into the environment (Everaert, 2018). The here developed ARM can be combined with plastic accumulation and distribution models (ADM) to improve plastic environmental risk assessment at the local and global scale. At TNO, Schwarz et al. (2023) implemented the often-used Material Flow Analysis (MFA) with the development of an ADM. This new approach included

plastic degradation rates and fate (transportation) in the environment, allowing a more thorough assessment of plastic litter's environmental impact. On this ground, combining ADM with ARM presents a promising new avenue to include additive loss in plastic environmental risk assessment. Adopting the ADM + ARM method in plastic risk assessment would establish a comprehensive framework to address additive toxicity, plastic pollution, impact assessment, and regulatory policymaking.

In a broader context, the developed ARM lays the foundation for estimating additive losses from plastic litter in different environmental compartments, addressing a notable gap in current research. The frequent omission of additives and their release into the environment in ERA studies often stems from the multiple complexities that hamper the development of accurate and applicable mathematical models to predict additive release(da Costa et al., 2024; MacLeod et al., 2023). These complexities encompass additive release kinetics and the limited and scattered available information on additive chemicals. Moreover, the multitude of physicochemical and environmental factors influencing additives, along with the diverse environmental compartments serving as plastic accumulation hotspots, further contribute to the complexity of the system. In this context, only a few studies have developed theoretical models for the prediction of additive loss in the surrounding environments (Feng, 2020; Lee et al., 2018; Sun et al., 2019).

Furthermore, in most cases, the reliability of existing models on empirical estimations limits their applicability and combination with existing models on plastic accumulation and distribution, such as the ones built by Kawecki & Nowack (2019) or Schwarz et al. (2023). As a result, most plastic impact assessment studies and regulation policies overlook plastic additives or merely focus on a limited number of well-known and frequently used chemicals (Bergmann et al., 2022; Lebreton et al., 2018; Martin et al., 2017; Matsuguma et al., 2017; Napper et al., 2020; Nawab et al., 2023), providing a biased and incomplete assessment of the plastic problem and its ecological impact.

In significant contrast, several mathematical models have been developed around food-contact materials and additive release (Begley et al., 2005; Hamdani et al., 1997; Petrosino et al., 2023; Poças et al., 2012; Reynier et al., 2002; Vitrac et al., 2007; Vitrac & Hayert, 2020). The accelerated progress around food-related polymers is facilitated by the progressive inclusion of new and more strict regulations on food safety and the demand for higher recycling rates of single-use packaging products. Additionally, the availability of detailed and constantly updated datasets on additives with reported human-related toxicity also eases the progress in this area.

Despite the high complexity and accuracy of most mathematical models on food-contact materials, their applicability for environmental purposes is limited. Models for food-contact materials operate by analyzing the migration of additives from packaging materials into food. Beyond their complexity, these models often include variables not considered in environmental-based models (i.e., the geometry of the packaging, the type of food, its texture, and total volume) (Petrosino et al., 2023; Reynier et al., 2002; Vitrac et al., 2007). For instance, in food-contact models, the shape and structure of packaging materials play a crucial role. In significant contrast, in environmentally-focused models, the priority lies in the release of additives from MNPs in light of the degradation process plastics undergo in the environment (Allan et al., 2022). Additionally, in ecological compartments, the surrounding environmental phase is presumed to act as an “infinite” sink (Feng, 2020; Sun et al., 2019). In the ARM, this is reflected in Assumption 7. In contrast, given the relatively small size of food items, their volume capacity is significantly reduced and should be considered as “finite”. Indeed, as described by Hadami et al. (1996), considering food as “infinite” may lead to overestimations. Finally, since food is ideally only maintained over relatively short periods before its consumption or disposal, the time framework considered in food-contact models is commonly shorter (Vitrac et al., 2007). These conditions contrast with the extensive periods plastic polymers stay in the environment before their

complete degradation. Combined, these disparities evidence the limited applicability of food contact models for environmental purposes, emphasizing the necessity of tailored-made models such as our ARM to address additive release in ecological compartments.

3. The use of ARM to improve plastic environmental risk assessment (ERA)

The ARM designed in this study is the first proof of concept for additive release from plastics in the environment. It provides a crucial step towards a more complete plastic environmental risk assessment (ERA).

Environmental Risk Assessment (ERA) studies aim to evaluate the potential environmental damage caused by toxic substances, activities, or natural events. The objective of ERA is to provide a scientific foundation for decision-making regarding the management, regulation, or mitigation of risks associated with the presence or release of substances in the environment (EFSA, accessed February 2024).

The imperative need to include additive release in plastic ERA studies

To date, a solid batch of studies have evidenced the occurrence of well-known toxic additives in the environment (Adjei et al., 2021; Han et al., 2018; Hermabessiere et al., 2017; Lu et al., 2023; Mukhopadhyay & Chakraborty, 2021; Schmidt et al., 2020; J. Wang et al., 2015; Zheng et al., 2024). For instance, (Zheng et al., 2024) described high levels of bisphenol A (BPA) and bis(2-ethylhexyl) phthalate (DEHP) in e-waste soil and agricultural soils surrounding e-waste landfills in the region of Agbogbloshie (Ghana). High levels of BPA and DHEP have also been found in the lower stretch of River Ganga (Mukhopadhyay & Chakraborty, 2021), significant levels of PBDEs have been detected near e-waste areas in China (Leung et al., 2011), and relevant concentrations of DEHP and TCPP (Tris(1-chloro-2-propyl) phosphate) in the Rhone River (France). In every instance, the studied areas were known to accumulate substantial amounts of plastic litter, whether in a controlled or uncontrolled manner. Combined, these observations evidence the strong correlation between the accumulation of plastic litter in particular areas and the presence of potentially toxic additives. Taking it one step further, it is paramount to draw attention to the impact that constant exposure to toxic additives can have on human health (Adeniran et al., 2022; Adjei et al., 2021; Awuchi et al., 2019; Linares et al., 2015; Meeker et al., 2009). Therefore, plastic litter and the release of associated additives must also be acknowledged as a societal issue, with adverse effects impacting both human health and environmental systems.

It is thereby evident that studies investigating the environmental impact of plastic cannot fully comprehend the risks to human health and the environment without accounting for additives and their rates of release. Moreover, the abovementioned studies also highlight the significant impact of plastics and related additives in different regions worldwide. Particular attention should be given to areas with limited or no ecosystem services and inadequate plastic waste management facilities. These areas may experience high rates of uncontrolled plastic loss and accumulation, ultimately leading to elevated levels of human and environmental exposure(Conlon, 2000; Owens & Conlon, 2021).

The role of the ARM in ERA studies

To shortly describe the ERA approach, hazard and exposure assessments are executed to evaluate chemical risks to human health and ecosystems. Hazard assessment involves evaluating a

chemical's inherent properties and its potential to cause harm, often using predicted non-effect concentrations (PNECs) derived from dose-response ecotoxicity tests (Hahn et al., 2014; Jung et al., 2021). Exposure assessment estimates environmental emissions and exposure to the substance, resulting in predicted environmental concentrations (PECs) in ecological compartments. PEC values are typically derived from field observations or modeling calculations. By comparing the predicted environmental concentration (PEC) to the predicted no-effect concentration (PNEC), the risk quotient (RQ) can be estimated (Figure 11). The RQ determines the environmental risk of a substance. A PEC/PNEC ratio exceeding 1 indicates concern. Typically, PEC and PNEC are measured in mg/L or mg/kg (Backhaus & Faust, 2012; Hahn et al., 2014; Jung et al., 2021; Nika et al., 2020; Peterson, 2006).

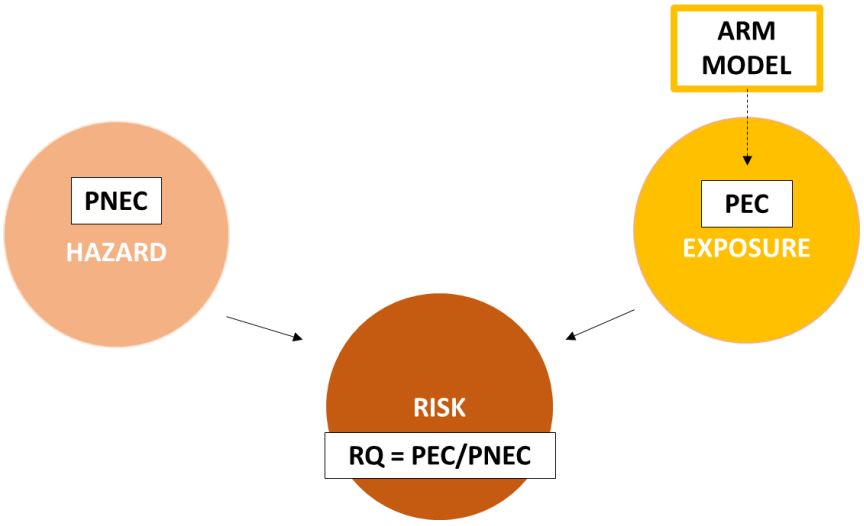

Figure 11. *The environmental risk of a substance is calculated using the so-called risk quotient (RQ) through the comparison of the predicted environmental concentration (PEC) against the predicted no-effect concentration (PNEC) of the substance; RQ=PEC/PNEC. If the PEC/PNEC ratio is greater than 1, the substance is considered of concern.*

The developed ARM allows the prediction of PEC values for selected target additives, combined with additive concentration and plastic accumulation numbers. The ARM results present the additive mass fraction (%) that is released from a specific polymer of a certain size under given conditions of time and temperature [100-(F%)], estimated with Equation (8). By combining the estimated [100-(F%)] with additive concentration values for a given polymer, the amount of additive released into the environment under specific given conditions can be calculated. These estimations can be combined with plastic pollution quantities in a particular environment, and the fraction that degrades to MNPs over time due to degradation. Hence, the ARM enables the derivation of predicted environmental concentrations (PEC, g/L) through ARM [100-(F%)] estimations, making it a valuable exposure assessment tool for addressing additive environmental toxicity.

However, a certain degree of overestimation (%) on additive release predictions is possible when using worst-case scenario Diffusion Coefficient (D*p) values derived from Piringer's Equation (Eq. 3). Based on D*p, the model predicts the worst-case scenario estimations for additive loss from polymers. Yet, assessing environmental risks under worst-case scenarios facilitates informed decision-making processes. It raises awareness of potential threats and prompts organizations and policymakers to consider the full spectrum of potential impacts. Therefore, the use of the ARM would result in the prioritization of actions that minimize additive harm to the environment and human health when introduced in plastic environmental risk assessment studies.

LIMITATIONS AND FUTURE PERSPECTIVES

In this study, an ARM was developed to model additive release rates from MNPs in aquatic environments. As a first proof of concept, the ARM was applied to estimate the release of four PBDEs from SBS, PP, PA, and HIPs. However, the reliability of our input dataset came into question given the inaccuracy of certain assumptions. Such assumptions were introduced to overcome the low data availability of certain parameters and the time limitations. Nevertheless, the author is aware of the uncertainties that may have arisen in this regard and the modeled ARM output was evaluated in consequence. A clear distinction was made between the model's qualitative performance and its accuracy in reproducing empirical estimations while using our input dataset. Nonetheless, additional important limitations and uncertainties must be highlighted.

The ARM model is only applicable to estimate additive release from amorphous polymers. According to Crank (1975), additive diffusivity and mass transport kinetics in crystalline (i.e. non-amorphous or glassy) and semi-crystalline polymers cannot be described by Fick's second. Additive diffusion processes in non-amorphous polymers are often affected by mechanisms such as relaxation processes, chain hopping, or localized transport within the matrix. These mechanisms result in deviations from the classic Fickian diffusion model, where the diffusion rate is solely dependent on concentration gradients. As Fick's second law describes a concentration-dependent diffusion (i.e. Fickian diffusion) driven by a constant negative concentration gradient, additive loss from non-amorphous polymers needs the consideration of alternative diffusion models (Crank, 1975; Feng, 2020). Nevertheless, while the ARM can't be applied to estimate additive loss from crystalline polymers, semi-crystalline plastics can be included under certain constraints. Semi-crystalline polymers consist of alternating regions of amorphous and non-amorphous sections within the matrix. Thereby, ARM additive release would solely estimate additive loss from the amorphous phase. To correct this, deep research must be performed to establish the amorphous-crystalline ratio of the material. However, in the context of this project, this correction was not included in the ARM due to time limitations. A homogeneous and constant additive distribution within the polymer was assumed. Thereby, the here estimated additive release rates for PA and PP, both semi-crystalline, should be regarded as an overestimation.

We presumed that the inconsistencies in the externally-controlled (Bi<1) additive release output might have arisen either from the mathematical solution to Fick's law or from inaccuracies in the input dataset. Although we do not rule out possible errors in the mathematical solution, the same solution has been successfully used previously in the literature (Feng, 2020). A tentative explanation is the use of the parameter octanol-water partitioning coefficient (Kow) instead of the plastic-water partitioning coefficient (Kpw). For instance, O'Connor et al. (2016) reported Kpw values of 5.61 and 6.9 for decaBDE (BDE209) and pentaBDE (BDE99), respectively. In contrast, the Kow used in this study for decaBDE and pentaBDE were 6.26 and 6.80, respectively. Higher partitioning coefficient values indicate a higher affinity of the additive for the organic phase, in this case, the polymer. Therefore, it may be conceivable that our Kow values contributed to underestimations in the additive partitioning rates, leading to the neglect of additive release rates (0%). Nonetheless, we cannot dismiss other potential factors, including the utilization of the sphere's radius for the water-boundary layer.

To correct the potential inaccuracies arising from the use of Kow coefficients, the inclusion of a mathematical solution to estimate Kpw values in our model should be considered in our model. Preliminary research on the topic led to the work of (Mosca Angelucci & Tomei, 2022) as a promising first approach to this matter. In this study, different mathematical approximations are described for the prediction of the partitioning equilibrium between the environmental phase and the polymer. Yet, such approximations must be carefully evaluated as they rely on the availability of the parameters.

Additionally, the ARM presumed no presence of environmental organic pollutants or dissolved organic matter in the aqueous medium. In the case of organic pollutants (OP), they are known to sorpt to the polymeric surface, influencing the desorption rate of additive release. This sorption of environmental pollutants is hypothesized to restrict or facilitate additive loss into the environment (Agboola & Benson, 2021; da Costa et al., 2024). In this context, real-world additive loss must be expected to differ from ARM estimations. In future studies, it would be of interest to consider additive-OP and polymer-OP interactions with well-defined groups of commonly found environmental organic chemicals (Zhu et al., 2021). The kinetics of these interactions could be included in the ARM as an additional parameter seeking to implement the accuracy and complexity of the model.

The model assumes that the considered MNPs do not further degrade over time. In this line, it is assumed that additive concentration within the MNPs would equal that present on the polymers upon manufacturing. Consequently, the model disregards the gradual degradation of polymers and the resulting release of additives as they age. Both processes have been consistently described in the literature (Cao et al., 2023; P. Liu et al., 2020; Luo et al., 2022; Ter Halle et al., 2016). UV light exposure is known to promote polymer aging, enhancing the fragmentation of the material into smaller particles (Conradie et al., 2022; Rummel et al., 2019; Viljoen et al., 2023). In this regard, work is currently underway to introduce plastic's degradation rates under UV light conditions (displayed in Annex 8) in the ARM.

Beyond UV light exposure, this first version of the ARM also overlooks other important environmental parameters such as microbial activity, organisms intake, or the hydrostatic pressure found at the sediment level (Ateia et al., 2020; Chen et al., 2023; H. Liu et al., 2020; Rani et al., 2017). These factors were dismissed for the sake of simplicity. Enhanced additive release in biotic conditions has been consistently reported in previous studies (Fauvelle et al., 2021; Lin et al., 2022; Paluselli et al., 2019). The lower pH conditions of the gastric fluids are known to activate additive release mobilization upon organism intake (Bakir et al., 2014; Li et al., 2019). As a final remark, the increased hydrostatic pressure observed at sediment levels in aquatic environments is recognized to reduce additive release due to the narrowing of pore diameters (Fauvelle et al., 2021). Thus, to adapt the ARM for plastic litter accumulating at the bottom of aquatic ecosystems, it is advisable to consider incorporating the factor of hydrostatic pressure in future studies.

Thereby, following a careful implementation of this first version of the ARM model, future research should focus on the inclusion of additional key parameters that were overlooked in the here presented ARM. This gradual inclusion of new variables will enhance the complexity of the ARM, resulting in a more reliable and accurate representation of the real-world system we aim to analyze.

CONCLUSION

In this study, an additive release model (ARM) was built based on a preliminary conceptual model. Additive release kinetics were translated into algorithms based on existing models, and a set of well-defined parameters was included, namely temperature, time, water presence, polymer type, polymer size, and additive molecular weight. The estimations of decaBDE release from ABS modeled by the ARM using empirical Dp estimations were in good agreement with those reported by Sun et al. (2019), serving as a positive reference control. Additionally, additive release trends under varying conditions aligned with those described in the literature. These observations collectively suggest that the ARM can reliably estimate internally-controlled additive release based on empirical Dp values.

This project lays the foundation for a first ARM version to estimate additive losses from plastic litter in environmental compartments. In conjunction with ERA studies, the ARM establishes the groundwork to address additive toxicity, plastic pollution, impact assessment, and regulatory policymaking.

Recommendations for future studies include implementing more reliable criteria during the data collection process to ensure the quantitative reliability of ARM estimations. Furthermore, additional environmental and physicochemical factors should be included in future works to enhance the accuracy of the model.

ANNEXES

Annex 1.

Table 13. Collected literature on environmental and physicochemical factors governing additive release.

Ref.	Author, year	Title	Factors considered
1	Paluselli, 2019	Phthalate Release from Plastic Fragments and Degradation in Seawater	Microbial activity, UV light exposure, polymer size, polymer type, additive molecular weight (MW), polymer aging
2	Chen, 2023	Insight into chemical features of migrated additives from plastics and associated risks to estuarine ecosystem	Wave action, UV light exposure, polymer type, polymer size
3	Luo, 2022	Effects of aging on environmental behavior of plastic additives: Migration, leaching, and ecotoxicity	Additive MW, polymer size, time
4	Liu, 2020	Sunlight-mediated cadmium release from colored microplastics containing cadmium pigment in aqueous phase	Uv light exposure, polymer size, organic matter content (%OM), additive hydrophobicity
5	Ateia, 2020	Microplastics release precursors of chlorinated and brominated disinfection byproducts in water	UV light exposure
6	Manviri, 2017	Releasing of hexabromocyclododecanes from expanded polystyrenes in seawater - field and laboratory experiments	UV light exposure, temperature, microbial activity, wave action, salinity, polymer size
7	Lertsirisopon, 2009	Abiotic degradation of four phthalic acid esters in aqueous phase under natural sunlight irradiation	Organic matter content (%OM), UV light exposure, temperature, pH, aerobic/anaerobic biodegradation
8	Koelmans, 2014	Leaching of plastic additives to marine organisms	Organisms intake, polymer size, additive hydrophobicity
9	Sun, 2019	Releases of brominated flame retardants (BFRs) from microplastics in aqueous medium: Kinetics and molecular-size dependence of diffusion	Temperature, time, polymer size, polymer type, additive MW
10	Bakir, 2014	Enhanced desorption of persistent organic pollutants from microplastics under simulated physiological conditions	Organism intake, pH, temperature

11	Dimassi, 2023	Effect of temperature and sunlight on the leachability potential of BPA and phthalates from plastic litter under marine conditions	Temperature, time, UV light exposure, abrasion, polymer type, additive type,
12	Raju Maddela, 2023	Additives of plastics: Entry into the environment and potential risks to human and ecological health	Time, temperature, UV light, Organisms intake, aging proces
13	Li, 2019	The release and earthworm bioaccumulation of endogenous hexabromocyclododecanes (HBCDDs) from expanded polystyrene foam microparticles	Organisms intake, additive hydrophobicity, size
14	Fauvelle, 2021	Organic additive release from plastic to seawater is lower under deep-sea conditions	Water presence, hydrostatic pressure, microbial activity, polymer size
15	Takada, 2019	Degradation of Various Plastics in the Environment	Polymer aging, aquatic conditions, organisms ingestion, additive hydrophobicity, pH
16	John Allan, 2022	Examining the Relevance of the Microplastic-Associated Additive Fraction in Environmental Compartments	Polymer crystallinity, additive MW, polymer size, additive hydrophobicity
17	Askadskii, 2013	The Influence of the Degree of Crystallinity on the Glass Transition Temperature of Polymers	Polymer crystallinity
18	Hahladakis, 2018	An overview of chemical additives present in plastics: Migration, release, fate and environmental impact during their use, disposal and recycling	Additive MW, polymer type, polymer size, water presence, time, temperature
19	Viljoen, 2023	Leaching of phthalate acid esters from plastic mulch films and their degradation in response to UV irradiation and contrasting soil conditions	Time, UV light, temperature, additive MW, organic matter presence

Annex 2

Table 14. Collected literature on additive release kinetics, mass transport mechanisms, and mathematical models.

Ref.	Author, year	Title
20	John Allan, 2022	Examining the Relevance of the Microplastic-Associated Additive Fraction in Environmental Compartments
21	Lee, 2018	Desorption modeling of hydrophobic organic chemicals from plastic sheets using experimentally determined diffusion coefficients in plastics

22	Sun, 2019	Releases of brominated flame retardants (BFRs) from microplastics in aqueous medium: Kinetics and molecular-size dependence of diffusion
23	Raewyn, 2020	Uptake and Release Kinetics of Organic Contaminants Associated with Micro- and Nanoplastic Particles
24	Hahladakis, 2018	An overview of chemical additives present in plastics: Migration, release, fate and environmental impact during their use, disposal and recycling
25	Barrick, 2021	Plastic additives: Challenges in ecotox hazard assessment
26	Bridson, 2021	Leaching and extraction of additives from plastic pollution to inform environmental risk: A multidisciplinary review of analytical approaches
27	Kwon, 2020	Microplastics as a Vector of Hydrophobic Contaminants: Importance of Hydrophobic Additives
28	Feng, 2020	Modeling Releases of Polymer Additives from Microplastics into the Aqueous Environment
29	Crank 1975	The mathematics of diffusion
30	Karimi, 2011	Diffusion in Polymer Solids and Solutions
31	Dong, 2010	The diffusion and solubility of Irganox® 1098 in polyamide 6
32	Piringer, 1994	Evaluation of plastics for food packaging
33	Hamdami, 1997	Prediction of worst-case migration from packaging to food using mathematical models
34	Limm and Hollifield, 1996	Modeling of additive diffusion in polyolefins
35	Barnes, 2007	Chemical Migration and Food Contact Materials
36	Nguyen, 2013	A computer-aided methodology to design safe food packaging and related systems
37	Plastics Europe, 2021	Applicability of mathematical modelling for the estimation of specific migration of substances from plastics

Annex 3.

Table 15. Temperature-independent A*'p values and activation energies for the different polymers selected. Data collected from Plastics Europe (2021). (*) ABS data belongs to SBS. SBS data was collected from Plastics Europe (2021) and used to estimate additive release from ABS based on the similarity in composition between both polymers.

Polymer	A'*p (m2/s)	τ (K)
ABS (*)	10.5	0
HIPS	0	1
PP	13.1	1577
PA	2	0

Table 16. Estimated temperature-dependant A*p values based on Eq. (4).

Polymer	**A*p (0°C)**	**A*p (10°C)**	**A*p (25°C)**	**A*p (30°C)**	**A*p (40°C)**
ABS *	10.5	10.5	10.5	10.5	10.5
HIPS	-0.003660992	-0.003531697	-0.003354016	-0.003298697	-0.003193358
PP	7.326615413	7.530513862	7.810716083	7.897954808	8.064074725
PA	2	2	2	2	2

Annex 4.

Table 17. Cumulative % of additive released (100-F(%)) for ABS and PP MNPs sized 1µm over time under Bi <1.

Polymer	Additive	1 day	3 days	7 days	15 days	30 days	150 days	365 days
ABS	pentaBDE (BDE-99)	0.00	0.00	0.00	0.00	0.00	0.00	0.00
	OctaBDE	0.00	0.00	0.00	0.00	0.00	0.00	0.00
	DecaBDE (BDE -209)	0.00	0.00	0.00	0.00	0.00	0.00	0.00
	BTBPE	0.00	0.00	0.00	0.00	0.00	0.00	0.00
PP	pentaBDE (BDE-99)	0.00	0.00	0.00	0.00	0.00	0.00	0.00
	OctaBDE	0.00	0.00	0.00	0.00	0.00	0.00	0.00
	DecaBDE (BDE -209)	0.00	0.00	0.00	0.00	0.00	0.00	0.00
	BTBPE	0.00	0.00	0.00	0.00	0.00	0.00	0.00

Annex 5.

Table 18. Released mass fraction [1- F(%)] from ABS 500 µm when assuming internally-controlled diffusion (Bi>1) for additives and temperatures with Bi=1 (highlighted in green). Complete calculations can be found in the Sup. Excel, worksheet *F% 500um.*

Polymer	Additive	Temperature	1 DAY	3 DAYS	7 DAYS	15 DAYS	30 DAYS	150 DAYS	365 DAYS
ABS	pentaBDE	0°C	8.28	14.11	21.10	29.99	40.76	75.57	93.63
		10°C	15.92	26.66	38.97	53.60	69.42	98.31	99.99
		25°C	37.50	59.05	78.96	93.87	99.38	100.00	100.00
		30°C	47.99	72.60	90.99	98.98	99.98	100.00	100.00
		40°C	72.66	94.81	99.81	100.00	100.00	100.00	100.00
	OctaBDE	0°C	3.56	6.12	9.27	13.41	18.67	38.94	56.32
		10°C	6.93	11.84	17.78	25.40	34.77	66.92	87.31
		25°C	17.04	28.46	41.45	56.70	72.83	99.02	100.00
		30°C	22.38	36.88	52.72	70.09	86.02	99.96	100.00
		40°C	36.92	58.26	78.14	93.36	99.28	100.00	100.00
	DecaBDE	0°C	2.20	3.80	5.78	8.39	11.76	25.22	37.66
		10°C	4.31	7.40	11.18	16.13	22.38	45.92	65.11
		25°C	10.71	18.15	26.96	37.95	50.86	87.35	98.67
		30°C	14.16	23.81	35.00	48.53	63.64	96.31	99.93
		40°C	23.84	39.12	55.63	73.31	88.72	99.99	100.00
	BTBPE	0°C	5.26	9.01	13.59	19.54	26.98	54.15	74.71
		10°C	10.20	17.30	25.72	36.29	48.79	85.25	98.08
		25°C	24.69	40.43	57.31	75.12	90.14	99.99	100.00
		30°C	32.15	51.51	70.74	87.97	97.63	100.00	100.00
		40°C	51.57	76.78	93.76	99.54	100.00	100.00	100.00

Table 19. Released mass fraction [1- F(%)] from ABS 500 µm when assuming externally-controlled diffusion (Bi<1) for additives and temperatures with Bi=1 (highlighted in green). Complete calculations can be found in the Sup. Excel, worksheet F% 500um

Polymer	Additive	Temperature	1 DAY	3 DAYS	7 DAYS	15 DAYS	30 DAYS	150 DAYS	365 DAYS
ABS	pentaBDE	0°C	8.28	14.11	21.10	29.99	40.76	75.57	93.63
		10°C	15.92	26.66	38.97	53.60	69.42	98.31	99.99
		25°C	0.00	0.00	0.00	0.00	0.00	0.00	0.00
		30°C	0.00	0.00	0.00	0.00	0.00	0.00	0.00
		40°C	0.00	0.00	0.00	0.00	0.00	0.00	0.00
	OctaBDE	0°C	3.56	6.12	9.27	13.41	18.67	38.94	56.32
		10°C	6.93	11.84	17.78	25.40	34.77	66.92	87.31
		25°C	17.04	28.46	41.45	56.70	72.83	99.02	100.00
		30°C	22.38	36.88	52.72	70.09	86.02	99.96	100.00
		40°C	0.00	0.00	0.00	0.00	0.00	0.00	0.00
	DecaBDE	0°C	2.20	3.80	5.78	8.39	11.76	25.22	37.66
		10°C	4.31	7.40	11.18	16.13	22.38	45.92	65.11
		25°C	10.71	18.15	26.96	37.95	50.86	87.35	98.67
		30°C	14.16	23.81	35.00	48.53	63.64	96.31	99.93
		40°C	23.84	39.12	55.63	73.31	88.72	99.99	100.00
	BTBPE	0°C	5.26	9.01	13.59	19.54	26.98	54.15	74.71
		10°C	10.20	17.30	25.72	36.29	48.79	85.25	98.08
		25°C	0.00	0.00	0.00	0.00	0.00	0.00	0.00
		30°C	0.00	0.00	0.00	0.00	0.00	0.00	0.00
		40°C	0.00	0.00	0.00	0.00	0.00	0.00	0.00

Annex 6. Cumulative % of additive released ([1-F(%)]*100) from MNPs size 500 µm over time under Bi >1

The tables here displayed can be found in Supplementary Excel, worksheet *F% 500µm.*

A		ABS (500 µm)							
Polymer	**Additive**	**Temperature**	**1 DAY**	**3 DAYS**	**7 DAYS**	**15 DAYS**	**30 DAYS**	**150 DAYS**	**365 DAYS**
ABS (500µm)	pentaBDE	0°C	8.28	14.11	21.10	29.99	40.76	75.57	93.63
		10°C	15.92	26.66	38.97	53.60	69.42	98.31	99.99
		25°C	37.50	59.05	78.96	93.87	99.38	100.00	100.00
		30°C	47.99	72.60	90.99	98.98	99.98	100.00	100.00
		40°C	72.66	94.81	99.81	100.00	100.00	100.00	100.00
	OctaBDE	0°C	3.56	6.12	9.27	13.41	18.67	38.94	56.32
		10°C	6.93	11.84	17.78	25.40	34.77	66.92	87.31
		25°C	17.04	28.46	41.45	56.70	72.83	99.02	100.00
		30°C	22.38	36.88	52.72	70.09	86.02	99.96	100.00
		40°C	36.92	58.26	78.14	93.36	99.28	100.00	100.00
	DecaBDE	0°C	2.20	3.80	5.78	8.39	11.76	25.22	37.66
		10°C	4.31	7.40	11.18	16.13	22.38	45.92	65.11
		25°C	10.71	18.15	26.96	37.95	50.86	87.35	98.67
		30°C	14.16	23.81	35.00	48.53	63.64	96.31	99.93
		40°C	23.84	39.12	55.63	73.31	88.72	99.99	100.00
	BTBPE	0°C	5.26	9.01	13.59	19.54	26.98	54.15	74.71
		10°C	10.20	17.30	25.72	36.29	48.79	85.25	98.08
		25°C	24.69	40.43	57.31	75.12	90.14	99.99	100.00
		30°C	32.15	51.51	70.74	87.97	97.63	100.00	100.00
		40°C	51.57	76.78	93.76	99.54	100.00	100.00	100.00

B		HIPS (500 µm)							
Polymer	**Additive**	**Temperature**	**1 DAY**	**3 DAYS**	**7 DAYS**	**15 DAYS**	**30 DAYS**	**150 DAYS**	**365 DAYS**
HIPS (500µm)	pentaBDE	0°C	0.04	0.08	0.12	0.17	0.24	0.54	0.85
		10°C	0.09	0.15	0.23	0.34	0.48	1.07	1.66
		25°C	0.22	0.38	0.58	0.85	1.21	2.69	4.17
		30°C	0.29	0.51	0.78	1.14	1.61	3.58	5.55
		40°C	0.51	0.88	1.35	1.97	2.78	6.16	9.52
	OctaBDE	0°C	0.02	0.03	0.05	0.07	0.10	0.23	0.36
		10°C	0.04	0.06	0.10	0.14	0.20	0.45	0.71
		25°C	0.09	0.16	0.25	0.36	0.51	1.14	1.78
		30°C	0.13	0.22	0.33	0.48	0.68	1.53	2.37
		40°C	0.22	0.38	0.57	0.84	1.18	2.64	4.10
	DecaBDE	0°C	0.02	0.02	0.03	0.04	0.06	0.14	0.22
		10°C	0.02	0.04	0.06	0.09	0.12	0.28	0.44
		25°C	0.06	0.10	0.15	0.22	0.32	0.71	1.10
		30°C	0.13	0.22	0.33	0.48	0.68	1.53	2.37
		40°C	0.13	0.23	0.35	0.52	0.73	1.63	2.54
	BTBPE	0°C	0.03	0.05	0.07	0.11	0.15	0.34	0.53
		10°C	0.05	0.10	0.15	0.21	0.30	0.67	1.05
		25°C	0.14	0.24	0.37	0.54	0.76	1.70	2.64
		30°C	0.19	0.32	0.49	0.72	1.01	2.26	3.51
		40°C	0.32	0.56	0.85	1.24	1.76	3.90	6.05

C

PP (500 µm)									
Polymer	**Additive**	**Temperature**	**1 DAY**	**3 DAYS**	**7 DAYS**	**15 DAYS**	**30 DAYS**	**150 DAYS**	**365 DAYS**
PP (500µm)	pentaBDE	0°C	1.73	2.98	4.53	6.59	9.26	20.05	30.24
		10°C	3.74	6.42	9.72	14.05	19.54	40.61	58.47
		25°C	10.67	18.08	26.85	37.81	50.69	87.18	98.63
		30°C	14.71	24.69	36.24	50.12	65.48	97.07	99.96
		40°C	26.69	43.46	61.12	79.09	92.95	100.00	100.00
	OctaBDE	0°C	0.73	1.27	1.94	2.83	3.98	8.79	13.53
		10°C	1.59	2.75	4.19	6.10	8.56	18.60	28.13
		25°C	4.60	7.90	11.93	17.20	23.82	48.55	68.28
		30°C	6.39	10.93	16.42	23.52	32.29	63.02	83.82
		40°C	11.86	20.04	29.66	41.55	55.31	91.25	99.46
	DecaBDE	0°C	0.45	0.78	1.20	1.75	2.47	5.47	8.47
		10°C	0.98	1.70	2.59	3.79	5.33	11.71	17.93
		25°C	2.85	4.91	7.46	10.81	15.10	31.97	47.03
		30°C	3.97	6.82	10.32	14.90	20.70	42.80	61.25
		40°C	7.41	12.64	18.95	27.03	36.91	70.13	89.89
	BTBPE	0°C	1.09	1.88	2.87	4.18	5.88	12.90	19.71
		10°C	2.36	4.07	6.18	8.98	12.57	26.87	39.99
		25°C	6.79	11.60	17.42	24.91	34.13	65.92	86.45
		30°C	9.01	15.33	22.87	32.42	43.89	79.62	95.84
		40°C	17.32	28.89	42.04	57.43	73.62	99.15	100.00

D

PA (500 µm)									
Polymer	**Additive**	**Temperature**	**1 DAY**	**3 DAYS**	**7 DAYS**	**15 DAYS**	**30 DAYS**	**150 DAYS**	**365 DAYS**
PA (500µm)	pentaBDE	0°C	0.12	0.21	0.32	0.47	0.66	1.47	2.29
		10°C	0.24	0.41	0.63	0.92	1.30	2.89	4.48
		25°C	0.60	1.04	1.58	2.31	3.26	7.22	11.14
		30°C	0.80	1.39	2.11	3.08	4.35	9.58	14.72
		40°C	1.39	2.40	3.65	5.32	7.47	16.29	24.75
	OctaBDE	0°C	0.05	0.09	0.14	0.20	0.28	0.63	0.98
		10°C	0.10	0.17	0.27	0.39	0.55	1.23	1.92
		25°C	0.25	0.44	0.67	0.99	1.39	3.10	4.81
		30°C	0.34	0.59	0.90	1.31	1.86	4.13	6.40
		40°C	0.59	1.02	1.56	2.27	3.21	7.10	10.95
	DecaBDE	0°C	0.03	0.05	0.08	0.12	0.17	0.39	0.60
		10°C	0.06	0.11	0.16	0.24	0.34	0.76	1.18
		25°C	0.16	0.27	0.42	0.61	0.86	1.92	2.98
		30°C	0.21	0.36	0.56	0.81	1.15	2.56	3.97
		40°C	0.36	0.63	0.96	1.41	1.99	4.41	6.84
	BTBPE	0°C	0.08	0.13	0.20	0.29	0.42	0.93	1.45
		10°C	0.15	0.26	0.40	0.58	0.82	1.82	2.84
		25°C	0.38	0.65	1.00	1.46	2.06	4.58	7.10
		30°C	0.50	0.87	1.33	1.95	2.75	6.09	9.41
		40°C	0.87	1.51	2.31	3.36	4.74	10.43	16.01

Annex 7. Cumulative % of additive released from ([1-F(%)]*100) MNPs size 1 µm over time under Bi>1

The tables here displayed can be found in Supplementary Excel, worksheet *F% 1µm*.

A			ABS (1 µm)						
Polymer	**Additive**	**Temperature**	**1 DAY**	**3 DAYS**	**7 DAYS**	**15 DAYS**	**30 DAYS**	**150 DAYS**	**365 DAYS**
ABS (SBS)	pentaBDE	0°C	100.00	100.00	100.00	100.00	100.00	100.00	100.00
		10°C	100.00	100.00	100.00	100.00	100.00	100.00	100.00
		25°C	100.00	100.00	100.00	100.00	100.00	100.00	100.00
		30°C	100.00	100.00	100.00	100.00	100.00	100.00	100.00
		40°C	100.00	100.00	100.00	100.00	100.00	100.00	100.00
	OctaBDE	0°C	100.00	100.00	100.00	100.00	100.00	100.00	100.00
		10°C	100.00	100.00	100.00	100.00	100.00	100.00	100.00
		25°C	100.00	100.00	100.00	100.00	100.00	100.00	100.00
		30°C	100.00	100.00	100.00	100.00	100.00	100.00	100.00
		40°C	100.00	100.00	100.00	100.00	100.00	100.00	100.00
	DecaBDE	0°C	100.00	100.00	100.00	100.00	100.00	100.00	100.00
		10°C	100.00	100.00	100.00	100.00	100.00	100.00	100.00
		25°C	100.00	100.00	100.00	100.00	100.00	100.00	100.00
		30°C	100.00	100.00	100.00	100.00	100.00	100.00	100.00
		40°C	100.00	100.00	100.00	100.00	100.00	100.00	100.00
	BTBPE	0°C	100.00	100.00	100.00	100.00	100.00	100.00	100.00
		10°C	100.00	100.00	100.00	100.00	100.00	100.00	100.00
		25°C	100.00	100.00	100.00	100.00	100.00	100.00	100.00
		30°C	100.00	100.00	100.00	100.00	100.00	100.00	100.00
		40°C	100.00	100.00	100.00	100.00	100.00	100.00	100.00

B			HIPS (1 µm)						
Polymer	**Additive**	**Temperature**	**1 DAY**	**3 DAYS**	**7 DAYS**	**15 DAYS**	**30 DAYS**	**150 DAYS**	**365 DAYS**
HIPS	pentaBDE	0°C	21.19	35.02	50.28	67.30	83.52	99.91	100.00
		10°C	39.13	61.28	81.21	95.16	99.62	100.00	100.00
		25°C	79.18	97.63	99.97	100.00	100.00	100.00	100.00
		30°C	91.15	99.81	100.00	100.00	100.00	100.00	100.00
		40°C	99.82	100.00	100.00	100.00	100.00	100.00	100.00
	OctaBDE	0°C	9.31	15.83	23.60	33.42	45.16	81.17	96.55
		10°C	17.86	29.76	43.22	58.88	75.16	99.36	100.00
		25°C	41.62	64.59	84.37	96.72	99.82	100.00	100.00
		30°C	52.93	78.30	94.65	99.67	100.00	100.00	100.00
		40°C	78.37	97.35	99.96	100.00	100.00	100.00	100.00
	DecaBDE	0°C	5.80	9.94	14.96	21.46	29.55	58.54	79.41
		10°C	11.23	19.01	28.19	39.60	52.91	89.25	99.11
		25°C	27.08	44.04	61.83	79.81	93.41	100.00	100.00
		30°C	52.93	78.30	94.65	99.67	100.00	100.00	100.00
		40°C	55.85	81.42	96.23	99.84	100.00	100.00	100.00
	BTBPE	0°C	13.65	22.98	33.83	47.02	61.87	95.47	99.89
		10°C	25.84	42.17	59.50	77.44	91.83	100.00	100.00
		25°C	57.52	83.11	96.98	99.90	100.00	100.00	100.00
		30°C	70.98	93.86	99.71	100.00	100.00	100.00	100.00
		40°C	93.90	99.94	100.00	100.00	100.00	100.00	100.00

C			PP (1 µm)						
Polymer	**Additive**	**Temperature**	**1 DAY**	**3 DAYS**	**7 DAYS**	**15 DAYS**	**30 DAYS**	**150 DAYS**	**365 DAYS**
PP	pentaBDE	0°C	100.00	100.00	100.00	100.00	100.00	100.00	100.00
		10°C	100.00	100.00	100.00	100.00	100.00	100.00	100.00
		25°C	100.00	100.00	100.00	100.00	100.00	100.00	100.00
		30°C	100.00	100.00	100.00	100.00	100.00	100.00	100.00
		40°C	100.00	100.00	100.00	100.00	100.00	100.00	100.00
	OctaBDE	0°C	100.00	100.00	100.00	100.00	100.00	100.00	100.00
		10°C	100.00	100.00	100.00	100.00	100.00	100.00	100.00
		25°C	100.00	100.00	100.00	100.00	100.00	100.00	100.00
		30°C	100.00	100.00	100.00	100.00	100.00	100.00	100.00
		40°C	100.00	100.00	100.00	100.00	100.00	100.00	100.00
	DecaBDE	0°C	99.37	100.00	100.00	100.00	100.00	100.00	100.00
		10°C	100.00	100.00	100.00	100.00	100.00	100.00	100.00
		25°C	100.00	100.00	100.00	100.00	100.00	100.00	100.00
		30°C	100.00	100.00	100.00	100.00	100.00	100.00	100.00
		40°C	100.00	100.00	100.00	100.00	100.00	100.00	100.00
	BTBPE	0°C	100.00	100.00	100.00	100.00	100.00	100.00	100.00
		10°C	100.00	100.00	100.00	100.00	100.00	100.00	100.00
		25°C	100.00	100.00	100.00	100.00	100.00	100.00	100.00
		30°C	100.00	100.00	100.00	100.00	100.00	100.00	100.00
		40°C	100.00	100.00	100.00	100.00	100.00	100.00	100.00

D			PA (1 µm)						
Polymer	**Additive**	**Temperature**	**1 DAY**	**3 DAYS**	**7 DAYS**	**15 DAYS**	**30 DAYS**	**150 DAYS**	**365 DAYS**
PA	pentaBDE	0°C	51.48	76.68	93.70	99.53	100.00	100.00	100.00
		10°C	82.50	98.58	99.99	100.00	100.00	100.00	100.00
		25°C	99.98	100.00	100.00	100.00	100.00	100.00	100.00
		30°C	100.00	100.00	100.00	100.00	100.00	100.00	100.00
		40°C	100.00	100.00	100.00	100.00	100.00	100.00	100.00
	OctaBDE	0°C	24.24	39.74	56.43	74.18	89.41	99.99	100.00
		10°C	44.29	68.03	87.41	97.93	99.93	100.00	100.00
		25°C	85.59	99.20	100.00	100.00	100.00	100.00	100.00
		30°C	95.36	99.97	100.00	100.00	100.00	100.00	100.00
		40°C	99.97	100.00	100.00	100.00	100.00	100.00	100.00
	DecaBDE	0°C	15.38	25.78	37.74	52.04	67.68	97.82	99.98
		10°C	28.94	46.83	65.23	83.11	95.35	100.00	100.00
		25°C	63.16	88.28	98.70	99.98	100.00	100.00	100.00
		30°C	76.87	96.78	99.94	100.00	100.00	100.00	100.00
		40°C	96.80	99.99	100.00	100.00	100.00	100.00	100.00
	BTBPE	0°C	34.71	55.17	74.83	91.13	98.71	100.00	100.00
		10°C	60.81	86.24	98.11	99.96	100.00	100.00	100.00
		25°C	97.47	100.00	100.00	100.00	100.00	100.00	100.00
		30°C	99.79	100.00	100.00	100.00	100.00	100.00	100.00
		40°C	100.00	100.00	100.00	100.00	100.00	100.00	100.00

Annex 8.

Table 20. Yearly degradation rate under UV light (percentile). Source (Schwarz et al.. 2023).

From	To	ABS	HIPS	PP	PA
Inland water	Inland water (MP)	0.01505	0.0004	0.0131	0.18
Wetland	Wetland (MP)	0.01505	0.0004	0.0131	0.18
Ocean	Ocean (MP)	0.01505	0.0004	0.0131	0.18

BIBLIOGRAPHY

Adeniran, A. A., Ayesu-Koranteng, E., & Shakantu, W. (2022). A Review of the Literature on the Environmental and Health Impact of Plastic Waste Pollutants in Sub-Saharan Africa. *Pollutants*, *2*(4), 531–545. https://doi.org/10.3390/pollutants2040034

Adjei, J. K., Ofori, A., Megbenu, H. K., Ahenguah, T., Boateng, A. K., Adjei, G. A., Bentum, J. K., & Essumang, D. K. (2021). Health risk and source assessment of semi-volatile phenols, p-chloroaniline and plasticizers in plastic packaged (sachet) drinking water. *Science of the Total Environment*, *797*. https://doi.org/10.1016/j.scitotenv.2021.149008

Adrian, S., Drisse, M. B., Cheng, Y., Devia, L., Deubzer, O., Goldizen, F., Gorman, J., Herat, S., Honda, S., Iattoni, G., Jingwei, W., Jinhui, L., Khetriwal, D. S., Linnell, J., Magalini, F., Nnororm, I. C., Onianwa, P., Ott, D., Ramola, A., … Zeng, X. (2020). *Quantities, flows, and the circular economy potential The Global E-waste Monitor 2020*.

Agboola, O. D., & Benson, N. U. (2021). Physisorption and Chemisorption Mechanisms Influencing Micro (Nano) Plastics-Organic Chemical Contaminants Interactions: A Review. In *Frontiers in Environmental Science* (Vol. 9). Frontiers Media S.A. https://doi.org/10.3389/fenvs.2021.678574

Alabi, O. A., Adeoluwa, Y. M., Huo, X., Xu, X., & Bakare, A. A. (2021). *Environmental contamination and public health effects of electronic waste: an overview*. https://doi.org/10.1007/s40201-021-00654-5/Published

Allan, I. J., Samanipour, S., Manoli, K., Gigault, J., & Fatta-Kassinos, D. (2022). Examining the Relevance of the Microplastic-Associated Additive Fraction in Environmental Compartments. *ACS Environmental Science and Technology Water*, *2*(3), 405–413. https://doi.org/10.1021/acsestwater.1c00310

Andrady, A. L., & Neal, M. A. (2009). Applications and societal benefits of plastics. *Philosophical Transactions of the Royal Society B: Biological Sciences*, *364*(1526), 1977–1984. https://doi.org/10.1098/rstb.2008.0304

Askadskii, A., Popova, M., Matseevich, T., & Kurskaya, E. (2014). The influence of the degree of crystallinity on the glass transition temperature of polymers. *Advanced Materials Research*, *864–867*, 751–754. https://doi.org/10.4028/www.scientific.net/AMR.864-867.751

Ateia, M., Kanan, A., & Karanfil, T. (2020). Microplastics release precursors of chlorinated and brominated disinfection byproducts in water. *Chemosphere*, *251*. https://doi.org/10.1016/j.chemosphere.2020.126452

Aurisano, N., Weber, R., & Fantke, P. (2021). Enabling a circular economy for chemicals in plastics. In *Current Opinion in Green and Sustainable Chemistry* (Vol. 31). Elsevier B.V. https://doi.org/10.1016/j.cogsc.2021.100513

Awere, E., Obeng, P. A., Bonoli, A., & Obeng, P. A. (2020). E-waste recycling and public exposure to organic compounds in developing countries: a review of recycling practices and toxicity levels in Ghana. In *Environmental Technology Reviews* (Vol. 9, Issue 1, pp. 1–19). Taylor and Francis Ltd. https://doi.org/10.1080/21622515.2020.1714749

Awuchi, C. G., Chinaza Godswill, A., & Godspel, A. C. (2019). Awuchi Chinaza Godswill, Awuchi Chibueze Godspel. Physiological Effects of Plastic Wastes on the Endocrine System. In *International Journal*

of Bioinformatics and Computational Biology (Vol. 4, Issue 2). http://www.aascit.org/journal/ijbcb

Backhaus, T., & Faust, M. (2012). Predictive environmental risk assessment of chemical mixtures: A conceptual framework. *Environmental Science and Technology*, *46*(5), 2564–2573. https://doi.org/10.1021/es2034125

Bakir, A., Rowland, S. J., & Thompson, R. C. (2014). Enhanced desorption of persistent organic pollutants from microplastics under simulated physiological conditions. *Environmental Pollution*, *185*, 16–23. https://doi.org/10.1016/j.envpol.2013.10.007

Barrick, A., Champeau, O., Chatel, A., Manier, N., Northcott, G., & Tremblay, L. A. (2021). Plastic additives: Challenges in ecotox hazard assessment. *PeerJ*, *9*. https://doi.org/10.7717/peerj.11300

Begley, T., Castle, L., Feigenbaum, A., Franz, R., Hinrichs, K., Lickly, T., Mercea, P., Milana, M., O'Brien, A., Rebre, S., Rijk, R., & Piringer, O. (2005). Evaluation of migration models that might be used in support of regulations for food-contact plastics. *Food Additives and Contaminants*, *22*(1), 73–90. https://doi.org/10.1080/02652030400028035

Bergmann, M., Collard, F., Fabres, J., Gabrielsen, G. W., Provencher, J. F., Rochman, C. M., van Sebille, E., & Tekman, M. B. (2022). Plastic pollution in the Arctic. In *Nature Reviews Earth and Environment* (Vol. 3, Issue 5, pp. 323–337). Springer Nature. https://doi.org/10.1038/s43017-022-00279-8

Bridson, J. H., Abbel, R., Smith, D. A., Northcott, G. L., & Gaw, S. (2023). Release of additives and non-intentionally added substances from microplastics under environmentally relevant conditions. *Environmental Advances*, *12*. https://doi.org/10.1016/j.envadv.2023.100359

Bridson, J. H., Gaugler, E. C., Smith, D. A., Northcott, G. L., & Gaw, S. (2021). Leaching and extraction of additives from plastic pollution to inform environmental risk: A multidisciplinary review of analytical approaches. In *Journal of Hazardous Materials* (Vol. 414). Elsevier B.V. https://doi.org/10.1016/j.jhazmat.2021.125571

Buekens, A., & Yang, J. (2014). Recycling of WEEE plastics: A review. In *Journal of Material Cycles and Waste Management* (Vol. 16, Issue 3, pp. 415–434). Springer Tokyo. https://doi.org/10.1007/s10163-014-0241-2

Cao, Z., Yi, J., Ding, Y., Sun, G., & Yu, J. (2023). Effects of aging degradation and reactive reconstruction on the structure and properties of styrene–butadiene–styrene block copolymer. *Construction and Building Materials*, *391*. https://doi.org/10.1016/j.conbuildmat.2023.131808

Chen, Q., Gao, Z., Wu, Y., Li, H., Jiang, J., Yang, Y., Xu, L., & Shi, H. (2023). Insight into chemical features of migrated additives from plastics and associated risks to estuarine ecosystem. *Journal of Hazardous Materials*, *448*. https://doi.org/10.1016/j.jhazmat.2023.130861

Conlon, K. (2000). *Waste Management in the Global South: an Inquiry on the Patterns of Plastic and Waste Material Flows in Colombo, Sri Lanka*. https://doi.org/10.15760/etd.7480

Conradie, W., Dorfling, C., Chimphango, A., Booth, A. M., Sørensen, L., & Akdogan, G. (2022). Investigating the Physicochemical Property Changes of Plastic Packaging Exposed to UV Irradiation and Different Aqueous Environments. *Microplastics*, *1*(3), 456–476. https://doi.org/10.3390/microplastics1030033

Costa, J. P. da, Avellan, A., Mouneyrac, C., Duarte, A., & Rocha-Santos, T. (2023). Plastic additives and microplastics as emerging contaminants: Mechanisms and analytical assessment. In *TrAC - Trends in Analytical Chemistry* (Vol. 158). Elsevier B.V. https://doi.org/10.1016/j.trac.2022.116898

Crank, J. (1975). *The mathematics of diffusion*. ISBN 9780198534112

da Costa, J. P., Avellan, A., Tubić, A., Duarte, A. C., & Rocha-Santos, T. (2024). Understanding Interface Exchanges for Assessing Environmental Sorption of Additives from Microplastics: Current Knowledge and Perspectives. In *Molecules (Basel, Switzerland)* (Vol. 29, Issue 2). https://doi.org/10.3390/molecules29020333

da Silva Müller Teixeira, F., de Carvalho Peres, A. C., Gomes, T. S., Visconte, L. L. Y., & Pacheco, E. B. A. V. (2021). A Review on the Applicability of Life Cycle Assessment to Evaluate the Technical and Environmental Properties of Waste Electrical and Electronic Equipment. In *Journal of Polymers and the Environment* (Vol. 29, Issue 5, pp. 1333–1349). Springer. https://doi.org/10.1007/s10924-020-01966-7

de Wit, C., Amelie, K., Niklas, R., & Ulla, S. (2010). *Emerging Brominated Flame Retardants in the Environment*.

Dimassi, S. N., Hahladakis, J. N., Yahia, M. N. D., Ahmad, M. I., Sayadi, S., & Al-Ghouti, M. A. (2023). Effect of temperature and sunlight on the leachability potential of BPA and phthalates from plastic litter under marine conditions. *Science of the Total Environment*, *894*. https://doi.org/10.1016/j.scitotenv.2023.164954

Dong, W., & Gijsman, P. (2010). The diffusion and solubility of Irganox® 1098 in polyamide 6. *Polymer Degradation and Stability*, *95*(6), 955–959. https://doi.org/10.1016/j.polymdegradstab.2010.03.020

Douziech, M., Benítez-López, A., Ernstoff, A., Askham, C., Hendriks, A. J., King, H., & Huijbregts, M. A. J. (2020). A regression-based model to predict chemical migration from packaging to food. *Journal of Exposure Science and Environmental Epidemiology*, *30*(3), 469–477. https://doi.org/10.1038/s41370-019-0185-7

EFSA, E.F.S.A. *Environmental Risk Assessment*. https://www.efsa.europa.eu/en/glossary/environmental-risk-assessment-era#:~:text=The%20process%20of%20assessing%20potential,the%20spread%20of%20plant%20pests. Accessed February 2024.

European Environment Agency. (2023, February 9). *Plastics, a growing environmental and climate concern: how can Europe revert that trend?*

Fauser, P., Vorkamp, K., & Strand, J. (2022). Residual additives in marine microplastics and their risk assessment – A critical review. In *Marine Pollution Bulletin* (Vol. 177). Elsevier Ltd. https://doi.org/10.1016/j.marpolbul.2022.113467

Fauvelle, V., Garel, M., Tamburini, C., Nerini, D., Castro-Jiménez, J., Schmidt, N., Paluselli, A., Fahs, A., Papillon, L., Booth, A. M., & Sempéré, R. (2021). Organic additive release from plastic to seawater is lower under deep-sea conditions. *Nature Communications*, *12*(1). https://doi.org/10.1038/s41467-021-24738-w

Feng, S. (2020). *Modeling Releases of Polymer Additives from Microplastics into the Aqueous Environment by*.

Filho, W. L., Salvia, A. L., Bonoli, A., Saari, U. A., Voronova, V., Klõga, M., Kumbhar, S. S., Olszewski, K., De Quevedo, D. M., & Barbir, J. (2021). An assessment of attitudes towards plastics and bioplastics in Europe. *Science of the Total Environment*, *755*. https://doi.org/10.1016/j.scitotenv.2020.142732

Forti, V., Kees, B., & Ruediger, K. (2018). *E-waste statistics guidelines on classification, reporting and indicators e-waste statistics guidelines on classification, reporting and indicators*. http://ewastemonitor.info/

Gallo, F., Fossi, C., Weber, R., Santillo, D., Sousa, J., Ingram, I., Nadal, A., & Romano, D. (2018). Marine litter plastics and microplastics and their toxic chemicals components: the need for urgent preventive measures. In *Environmental Sciences Europe* (Vol. 30, Issue 1). Springer Verlag. https://doi.org/10.1186/s12302-018-0139-z

Groh, K. J., Backhaus, T., Carney-Almroth, B., Geueke, B., Inostroza, P. A., Lennquist, A., Leslie, H. A., Maffini, M., Slunge, D., Trasande, L., Warhurst, A. M., & Muncke, J. (2019). Overview of known plastic packaging-associated chemicals and their hazards. In *Science of the Total Environment* (Vol. 651, pp. 3253–3268). Elsevier B.V. https://doi.org/10.1016/j.scitotenv.2018.10.015

Hahladakis, J. N., Velis, C. A., Weber, R., Iacovidou, E., & Purnell, P. (2018). An overview of chemical additives present in plastics: Migration, release, fate and environmental impact during their use, disposal and recycling. In *Journal of Hazardous Materials* (Vol. 344, pp. 179–199). Elsevier B.V. https://doi.org/10.1016/j.jhazmat.2017.10.014

Hahn, T., Diamond, J., Dobson, S., Howe, P., Kielhorn, J., Koennecker, G., Lee-Steere, C., Mangelsdorf, I., Schneider, U., Sugaya, Y., Taylor, K., Dam, R. Van, & Stauber, J. L. (2014). Predicted no effect concentration derivation as a significant source of variability in environmental hazard assessments of chemicals in aquatic systems: an international analysis. *Integrated Environmental Assessment and Management*, *10*(1), 30–36. https://doi.org/10.1002/ieam.1473

Hamdani, M., Feigenbaum, A., & Vergnaud, J. M. (1997). Prediction of worst case migration from packaging to food using mathematical models. *Food Additives and Contaminants*, *14*(5), 499–506. https://doi.org/10.1080/02652039709374557

Han, W., Gao, G., Geng, J., Li, Y., & Wang, Y. (2018). Ecological and health risks assessment and spatial distribution of residual heavy metals in the soil of an e-waste circular economy park in Tianjin, China. *Chemosphere*, *197*, 325–335. https://doi.org/10.1016/j.chemosphere.2018.01.043

Hayduk, W., & Laudie, H. (1974). *Prediction of Diffusion Coefficients for Nonelectrolytes in Dilute Aqueous Solutions*.

He, Z., Li, G., Chen, J., Huang, Y., An, T., & Zhang, C. (2015). Pollution characteristics and health risk assessment of volatile organic compounds emitted from different plastic solid waste recycling workshops. *Environment International*, *77*, 85–94. https://doi.org/10.1016/j.envint.2015.01.004

Hermabessiere, L., Dehaut, A., Paul-Pont, I., Lacroix, C., Jezequel, R., Soudant, P., & Duflos, G. (2017). Occurrence and effects of plastic additives on marine environments and organisms: A review. In *Chemosphere* (Vol. 182, pp. 781–793). Elsevier Ltd. https://doi.org/10.1016/j.chemosphere.2017.05.096

Hirai, H., Takada, H., Ogata, Y., Yamashita, R., Mizukawa, K., Saha, M., Kwan, C., Moore, C., Gray, H., Laursen, D., Zettler, E. R., Farrington, J. W., Reddy, C. M., Peacock, E. E., & Ward, M. W. (2011). Organic micropollutants in marine plastics debris from the open ocean and remote and urban

beaches. *Marine Pollution Bulletin*, *62*(8), 1683–1692. https://doi.org/10.1016/j.marpolbul.2011.06.004

International Labour Organization. (2014). *Tackling informality in e-waste management: The potential of cooperative enterprises*.

Izdebska, J., & Thomas, S. (2016). *Printing on Polymers*. ISBN: 9780323374682

J.S. Baughan. (2015). *Global Legislation for Food Contact Materials. Woodhead Publishing Series in Food Science, Technology and Nutrition.*

Jung, J. W., Kang, J. S., Choi, J., & Park, J. W. (2021). A novel approach to derive the predicted no-effect concentration (Pnec) of benzophenone-3 (bp-3) using the species sensitivity distribution (ssd) method: Suggestion of a new pnec value for bp-3. *International Journal of Environmental Research and Public Health*, *18*(7). https://doi.org/10.3390/ijerph18073650

Karimi, M. (2011). *Diffusion in Polymer Solids and Solutions*. www.intechopen.com

Kawecki, D., & Nowack, B. (2019). Polymer-Specific Modeling of the Environmental Emissions of Seven Commodity Plastics As Macro- and Microplastics. *Environmental Science and Technology*, *53*(16), 9664–9676. https://doi.org/10.1021/acs.est.9b02900

Kousaiti, A., Hahladakis, J. N., Savvilotidou, V., Pivnenko, K., Tyrovola, K., Xekoukoulotakis, N., Astrup, T. F., & Gidarakos, E. (2020). Assessment of tetrabromobisphenol-A (TBBPA) content in plastic waste recovered from WEEE. *Journal of Hazardous Materials*, *390*. https://doi.org/10.1016/j.jhazmat.2019.121641

Kruczek, B. (2015). Diffusion Coefficient. In *Encyclopedia of Membranes* (pp. 1–4). Springer Berlin Heidelberg. https://doi.org/10.1007/978-3-642-40872-4_1993-1

Kwon, J. H., Chang, S., Hong, S. H., & Shim, W. J. (2017). Microplastics as a vector of hydrophobic contaminants: Importance of hydrophobic additives. In *Integrated Environmental Assessment and Management* (Vol. 13, Issue 3, pp. 494–499). Wiley-Blackwell. https://doi.org/10.1002/ieam.1906

Lambert, S., & Wagner, M. (2017). Environmental performance of bio-based and biodegradable plastics: The road ahead. In *Chemical Society Reviews* (Vol. 46, Issue 22, pp. 6855–6871). Royal Society of Chemistry. https://doi.org/10.1039/c7cs00149e

Lebreton, L., Slat, B., Ferrari, F., Sainte-Rose, B., Aitken, J., Marthouse, R., Hajbane, S., Cunsolo, S., Schwarz, A., Levivier, A., Noble, K., Debeljak, P., Maral, H., Schoeneich-Argent, R., Brambini, R., & Reisser, J. (2018). Evidence that the Great Pacific Garbage Patch is rapidly accumulating plastic. *Scientific Reports*, *8*(1). https://doi.org/10.1038/s41598-018-22939-w

Lee, H., Byun, D. E., Kim, J. M., & Kwon, J. H. (2018). Desorption modeling of hydrophobic organic chemicals from plastic sheets using experimentally determined diffusion coefficients in plastics. *Marine Pollution Bulletin*, *126*, 312–317. https://doi.org/10.1016/j.marpolbul.2017.11.032

Leung, A. O. W., Zheng, J., Yu, C. K., Liu, W. K., Wong, C. K. C., Cai, Z., & Wong, M. H. (2011). Polybrominated diphenyl ethers and polychlorinated dibenzo- P -dioxins and dibenzofurans in surface dust at an E-waste processing site in southeast China. *Environmental Science and Technology*, *45*(13), 5775–5782. https://doi.org/10.1021/es103915w

Li, B., Lan, Z., Wang, L., Sun, H., Yao, Y., Zhang, K., & Zhu, L. (2019). The release and earthworm bioaccumulation of endogenous hexabromocyclododecanes (HBCDDs) from expanded polystyrene foam microparticles. *Environmental Pollution*, *255*. https://doi.org/10.1016/j.envpol.2019.113163

Limm, W., & Hollifield, H. C. (1996). Modelling of additive diffusion in polyolefins. *Food Additives and Contaminants*, *13*(8), 949–967. https://doi.org/10.1080/02652039609374482

Lin, Z., Jin, T., Zou, T., Xu, L., Xi, B., Xu, D., He, J., Xiong, L., Tang, C., Peng, J., Zhou, Y., & Fei, J. (2022). Current progress on plastic/microplastic degradation: Fact influences and mechanism. In *Environmental Pollution* (Vol. 304). Elsevier Ltd. https://doi.org/10.1016/j.envpol.2022.119159

Linares, V., Bellés, M., & Domingo, J. L. (2015). Human exposure to PBDE and critical evaluation of health hazards. In *Archives of Toxicology* (Vol. 89, Issue 3, pp. 335–356). Springer Verlag. https://doi.org/10.1007/s00204-015-1457-1

Liu, H., Liu, K., Fu, H., Ji, R., & Qu, X. (2020). Sunlight mediated cadmium release from colored microplastics containing cadmium pigment in aqueous phase. *Environmental Pollution*, *263*. https://doi.org/10.1016/j.envpol.2020.114484

Liu, P., Lu, K., Li, J., Wu, X., Qian, L., Wang, M., & Gao, S. (2020). Effect of aging on adsorption behavior of polystyrene microplastics for pharmaceuticals: Adsorption mechanism and role of aging intermediates. *Journal of Hazardous Materials*, *384*. https://doi.org/10.1016/j.jhazmat.2019.121193

Lu, R., Zhang, Y., Guo, K., He, Z., Yu, W., Cao, X., Zheng, X., & Mai, B. (2023). Organophosphate flame retardants and plastics in soil from an abandoned e-waste recycling site: significant ecological risks derived from plastic debris. *Environmental Science and Pollution Research*, *30*(20), 58933–58943. https://doi.org/10.1007/s11356-023-26625-x

Luo, H., Liu, C., He, D., Sun, J., Li, J., & Pan, X. (2022). Effects of aging on environmental behavior of plastic additives: Migration, leaching, and ecotoxicity. In *Science of the Total Environment* (Vol. 849). Elsevier B.V. https://doi.org/10.1016/j.scitotenv.2022.157951

MacLeod, M., Domercq, P., Harrison, S., & Praetorius, A. (2023). Computational models to confront the complex pollution footprint of plastic in the environment. *Nature Computational Science*, *3*(6), 486–494. https://doi.org/10.1038/s43588-023-00445-y

Mao, S., Gu, W., Bai, J., Dong, B., Huang, Q., Zhao, J., Zhuang, X., Zhang, C., Yuan, W., & Wang, J. (2020a). Migration characteristics of heavy metals during simulated use of secondary products made from recycled e-waste plastic. *Journal of Environmental Management*, *266*. https://doi.org/10.1016/j.jenvman.2020.110577

Mao, S., Gu, W., Bai, J., Dong, B., Huang, Q., Zhao, J., Zhuang, X., Zhang, C., Yuan, W., & Wang, J. (2020b). Migration characteristics of heavy metals during simulated use of secondary products made from recycled e-waste plastic. *Journal of Environmental Management*, *266*. https://doi.org/10.1016/j.jenvman.2020.110577

Martin, J., Lusher, A., Thompson, R. C., & Morley, A. (2017). The Deposition and Accumulation of Microplastics in Marine Sediments and Bottom Water from the Irish Continental Shelf. *Scientific Reports*, *7*(1). https://doi.org/10.1038/s41598-017-11079-2

Martinho, G., Pires, A., Saraiva, L., & Ribeiro, R. (2012). Composition of plastics from waste electrical and electronic equipment (WEEE) by direct sampling. *Waste Management*, *32*(6), 1213–1217. https://doi.org/10.1016/j.wasman.2012.02.010

Matsuguma, Y., Takada, H., Kumata, H., Kanke, H., Sakurai, S., Suzuki, T., Itoh, M., Okazaki, Y., Boonyatumanond, R., Zakaria, M. P., Weerts, S., & Newman, B. (2017). Microplastics in Sediment Cores from Asia and Africa as Indicators of Temporal Trends in Plastic Pollution. *Archives of Environmental Contamination and Toxicology*, *73*(2), 230–239. https://doi.org/10.1007/s00244-017-0414-9

Meeker, J. D., Sathyanarayana, S., & Swan, S. H. (2009). Phthalates and other additives in plastics: human exposure and associated health outcomes. *Philosophical Transactions of the Royal Society B: Biological Sciences*, *364*(1526), 2097–2113. https://doi.org/10.1098/rstb.2008.0268

Ministry of Environment and Food Denmark. (2016). *Fire safety requirements and alternatives to brominated flame-retardants : a LOUS follow-up project*. Miljøstyrelsen.

Mosca Angelucci, D., & Tomei, M. C. (2022). Uptake/release of organic contaminants by microplastics: A critical review of influencing factors, mechanistic modeling, and thermodynamic prediction methods. In *Critical Reviews in Environmental Science and Technology* (Vol. 52, Issue 8, pp. 1356–1400). Taylor and Francis Ltd. https://doi.org/10.1080/10643389.2020.1856594

Mukhopadhyay, M., & Chakraborty, P. (2021). Plasticizers and bisphenol A: Emerging organic pollutants along the lower stretch of River Ganga, north-east coast of the Bay of Bengal. *Environmental Pollution*, *276*. https://doi.org/10.1016/j.envpol.2021.116697

Napper, I. E., Davies, B. F. R., Clifford, H., Elvin, S., Koldewey, H. J., Mayewski, P. A., Miner, K. R., Potocki, M., Elmore, A. C., Gajurel, A. P., & Thompson, R. C. (2020). Reaching New Heights in Plastic Pollution—Preliminary Findings of Microplastics on Mount Everest. *One Earth*, *3*(5), 621–630. https://doi.org/10.1016/j.oneear.2020.10.020

Nawab, J., Khan, H., Ghani, J., Zafar, M. I., Khan, S., Toller, S., Fatima, L., & Hamza, A. (2023). New insights into the migration, distribution and accumulation of micro-plastic in marine environment: A critical mechanism review. *Chemosphere*, *330*. https://doi.org/10.1016/j.chemosphere.2023.138572

Nguyen, P. M., Goujon, A., Sauvegrain, P., & Vitrac, O. (2013a). A computer-aided methodology to design safe food packaging and related systems. *AIChE Journal*, *59*(4), 1183–1212. https://doi.org/10.1002/aic.14056

Nguyen, P. M., Goujon, A., Sauvegrain, P., & Vitrac, O. (2013b). A computer-aided methodology to design safe food packaging and related systems. *AIChE Journal*, *59*(4), 1183–1212. https://doi.org/10.1002/aic.14056

Nika, M. C., Ntaiou, K., Elytis, K., Thomaidi, V. S., Gatidou, G., Kalantzi, O. I., Thomaidis, N. S., & Stasinakis, A. S. (2020). Wide-scope target analysis of emerging contaminants in landfill leachates and risk assessment using Risk Quotient methodology. *Journal of Hazardous Materials*, *394*. https://doi.org/10.1016/j.jhazmat.2020.122493

Nnorom, I. C., & Osibanjo, O. (2008). Sound management of brominated flame retarded (BFR) plastics from electronic wastes: State of the art and options in Nigeria. In *Resources, Conservation and Recycling* (Vol. 52, Issue 12, pp. 1362–1372). https://doi.org/10.1016/j.resconrec.2008.08.001

O'Connor, I. A., Golsteijn, L., & Hendriks, A. J. (2016). Review of the partitioning of chemicals into different plastics: Consequences for the risk assessment of marine plastic debris. In *Marine Pollution Bulletin* (Vol. 113, Issues 1–2, pp. 17–24). Elsevier Ltd. https://doi.org/10.1016/j.marpolbul.2016.07.021

Owens, K. A., & Conlon, K. (2021). Mopping Up or Turning Off the Tap? Environmental Injustice and the Ethics of Plastic Pollution. *Frontiers in Marine Science*, *8*. https://doi.org/10.3389/fmars.2021.713385

Paluselli, A., Fauvelle, V., Galgani, F., & Sempéré, R. (2019). Phthalate Release from Plastic Fragments and Degradation in Seawater. *Environmental Science and Technology*, *53*(1), 166–175. https://doi.org/10.1021/acs.est.8b05083

Peterson, R. K. D. (2006). Comparing ecological risks of pesticides: The utility of a risk quotient ranking approach across refinements of exposure. *Pest Management Science*, *62*(1), 46–56. https://doi.org/10.1002/ps.1126

Petrosino, F., Coppola, G., Chakraborty, S., & Curcio, S. (2023). Modeling of specific migration from food contact materials. *Journal of Food Engineering*, *357*. https://doi.org/10.1016/j.jfoodeng.2023.111652

Petrovics, N., Kirchkeszner, C., Patkó, A., Tábi, T., Magyar, N., Kovácsné Székely, I., Szabó, B. S., Nyiri, Z., & Eke, Z. (2023). Effect of crystallinity on the migration of plastic additives from polylactic acid-based food contact plastics. *Food Packaging and Shelf Life*, *36*. https://doi.org/10.1016/j.fpsl.2023.101054

Pibul, P., Jawjit, S., & Yimthiang, S. (2023). Soil heavy metal pollution from waste electrical and electronic equipment of repair and junk shops in southern Thailand and their ecological risk. *Heliyon*, *9*(10). https://doi.org/10.1016/j.heliyon.2023.e20438

Piringer, O. G. (1994). Evaluation of Plastics for Food Packaging. *Food Additives and Contaminants*, *11*(2), 221–230. https://doi.org/10.1080/02652039409374220

Plastics Europe. (2021). *Applicability of mathematical modelling for the estimation of specific migration of substances from plastics*. http://ihcp.jrc.ec.europa.eu/

Plastics Europe. (2022). *Plastics - The Facts 2022. Enabling a Sustainable Future*. https://plasticseurope.org/knowledge-hub/plastics-the-facts-2022/

Poças, M. F., Oliveira, J. C., Brandsch, R., & Hogg, T. (2012). Analysis of mathematical models to describe the migration of additives from packaging plastics to foods. *Journal of Food Process Engineering*, *35*(4), 657–676. https://doi.org/10.1111/j.1745-4530.2010.00612.x

Rani, M., Shim, W. J., Jang, M., Han, G. M., & Hong, S. H. (2017). Releasing of hexabromocyclododecanes from expanded polystyrenes in seawater -field and laboratory experiments. *Chemosphere*, *185*, 798–805. https://doi.org/10.1016/j.chemosphere.2017.07.042

Reynier, A., Dole, P., & Feigenbaum, A. (2002). Migration of additives from polymers into food simulants: Numerical solution of a mathematical model taking into account food and polymer interactions. *Food Additives and Contaminants*, *19*(1), 89–102. https://doi.org/10.1080/02652030110051266

Rummel, C. D., Escher, B. I., Sandblom, O., Plassmann, M. M., Arp, H. P. H., Macleod, M., & Jahnke, A. (2019). Effects of Leachates from UV-Weathered Microplastic in Cell-Based Bioassays.

Environmental Science and Technology, *53*(15), 9214–9223. https://doi.org/10.1021/acs.est.9b02400

Rusina, T. P., Smedes, F., & Klanova, J. (2010). Diffusion coefficients of polychlorinated biphenyls and polycyclic aromatic hydrocarbons in polydimethylsiloxane and low-density polyethylene polymers. *Journal of Applied Polymer Science*, *116*(3), 1803–1810. https://doi.org/10.1002/app.31704

Rusina, T. P., Smedes, F., Klanova, J., Booij, K., & Holoubek, I. (2007). Polymer selection for passive sampling: A comparison of critical properties. *Chemosphere*, *68*(7), 1344–1351. https://doi.org/10.1016/j.chemosphere.2007.01.025

Schmidt, N., Castro-Jiménez, J., Fauvelle, V., Ourgaud, M., & Sempéré, R. (2020). Occurrence of organic plastic additives in surface waters of the Rhône River (France). *Environmental Pollution*, *257*. https://doi.org/10.1016/j.envpol.2019.113637

Schwarz, A. E., Lensen, S. M. C., Langeveld, E., Parker, L. A., & Urbanus, J. H. (2023). Plastics in the global environment assessed through material flow analysis, degradation and environmental transportation. *Science of the Total Environment*, *875*. https://doi.org/10.1016/j.scitotenv.2023.162644

Sheela, A. M., Manimekalai, B., & Dhinagaran, G. (2022). Review on the distribution of microplastics in the oceans and its impacts: Need for modeling-based approach to investigate the transport and risk of microplastic pollution. In *Environmental Engineering Research* (Vol. 27, Issue 4). Korean Society of Environmental Engineers. https://doi.org/10.4491/eer.2021.243

Stenmarck, Å., Belleza, E. L., Fråne, A., Busch, N., Larsen, Å., & Wahlström, M. (2017). *Hazardous substances in plastics-ways to increase recycling In cooperation with IVL Svenska Miljöinstitutet AB, CRI*, SINTEF**, VTT****. www.ivl.se

Stubbings, W. A., Abdallah, M. A. E., Misiuta, K., Onwuamaegbu, U., Holland, J., Smith, L., Parkinson, C., McKinlay, R., & Harrad, S. (2021). Assessment of brominated flame retardants in a small mixed waste electronic and electrical equipment (WEEE) plastic recycling stream in the UK. *Science of the Total Environment*, *780*. https://doi.org/10.1016/j.scitotenv.2021.146543

Sun, B., Hu, Y., Cheng, H., & Tao, S. (2019). Releases of brominated flame retardants (BFRs) from microplastics in aqueous medium: Kinetics and molecular-size dependence of diffusion. *Water Research*, *151*, 215–225. https://doi.org/10.1016/j.watres.2018.12.017

Tang, Z., Huang, Q., Yang, Y., Nie, Z., Cheng, J., Yang, J., Wang, Y., & Chai, M. (2016). Polybrominated diphenyl ethers (PBDEs) and heavy metals in road dusts from a plastic waste recycling area in north China: implications for human health. *Environmental Science and Pollution Research*, *23*(1), 625–637. https://doi.org/10.1007/s11356-015-5296-7

Tang, Z., Zhang, L., Huang, Q., Yang, Y., Nie, Z., Cheng, J., Yang, J., Wang, Y., & Chai, M. (2015). Contamination and risk of heavy metals in soils and sediments from a typical plastic waste recycling area in North China. *Ecotoxicology and Environmental Safety*, *122*, 343–351. https://doi.org/10.1016/j.ecoenv.2015.08.006

Tawfik A. Saleh. (2022). Interface Science and Technology, Volume:34C, Page(s):65-97. *Interface Science and Technology*.

Ter Halle, A., Ladirat, L., Gendre, X., Goudouneche, D., Pusineri, C., Routaboul, C., Tenailleau, C., Duployer, B., & Perez, E. (2016). Understanding the Fragmentation Pattern of Marine Plastic Debris. *Environmental Science and Technology*, *50*(11), 5668–5675. https://doi.org/10.1021/acs.est.6b00594

Teuten, E. L., Saquing, J. M., Knappe, D. R. U., Barlaz, M. A., Jonsson, S., Björn, A., Rowland, S. J., Thompson, R. C., Galloway, T. S., Yamashita, R., Ochi, D., Watanuki, Y., Moore, C., Viet, P. H., Tana, T. S., Prudente, M., Boonyatumanond, R., Zakaria, M. P., Akkhavong, K., … Takada, H. (2009). Transport and release of chemicals from plastics to the environment and to wildlife. *Philosophical Transactions of the Royal Society B: Biological Sciences*, *364*(1526), 2027–2045. https://doi.org/10.1098/rstb.2008.0284

Town, R. M., & Van Leeuwen, H. P. (2020). Uptake and Release Kinetics of Organic Contaminants Associated with Micro- A nd Nanoplastic Particles. *Environmental Science and Technology*, *54*(16), 10057–10067. https://doi.org/10.1021/acs.est.0c02297

Tsioptsias, N., Tako, A., & Robinson, S. (2016). Model validation and testing in simulation: A literature review. *OpenAccess Series in Informatics*, *50*, 6.1-6.11. https://doi.org/10.4230/OASIcs.SCOR.2016.6

UN United Nations. (2010). *Work programmes on new persistent organic pollutants as adopted by the Conference of the Parties* (Vol. 4).

UN Environment Program. (2016). *MARINE PLASTIC DEBRIS AND MICROPLASTICS Global lessons and research to inspire action and guide policy change Advance copy ii*.

Uzun, P., Farazande, S., & Guven, B. (2022a). Mathematical modeling of microplastic abundance, distribution, and transport in water environments: A review. In *Chemosphere* (Vol. 288). Elsevier Ltd. https://doi.org/10.1016/j.chemosphere.2021.132517

Uzun, P., Farazande, S., & Guven, B. (2022b). Mathematical modeling of microplastic abundance, distribution, and transport in water environments: A review. In *Chemosphere* (Vol. 288). Elsevier Ltd. https://doi.org/10.1016/j.chemosphere.2021.132517

Van Den Berg, M., Van De Meent, D., Peijnenburg, W. J. G. M., Sijm, D. T. H. M., Struijs, L., & Tas, L. W. (1995). *TRANSPORT, ACCUMULATION AND TRANSFORMATION PROCESSES*.

Viljoen, S. J., Brailsford, F. L., Murphy, D. V., Hoyle, F. C., Chadwick, D. R., & Jones, D. L. (2023). Leaching of phthalate acid esters from plastic mulch films and their degradation in response to UV irradiation and contrasting soil conditions. *Journal of Hazardous Materials*, *443*. https://doi.org/10.1016/j.jhazmat.2022.130256

Vitrac, O., & Hayert, M. (2020). Modeling in food across the scales: towards a universal mass transfer simulator of small molecules in food. *SN Applied Sciences*, *2*(9). https://doi.org/10.1007/s42452-020-03272-2

Vitrac, O., Mougharbel, A., & Feigenbaum, A. (2007). Interfacial mass transport properties which control the migration of packaging constituents into foodstuffs. *Journal of Food Engineering*, *79*(3), 1048–1064. https://doi.org/10.1016/j.jfoodeng.2006.03.030

Wang, J., Liu, L., Wang, J., Pan, B., Fu, X., Zhang, G., Zhang, L., & Lin, K. (2015). Distribution of metals and brominated flame retardants (BFRs) in sediments, soils and plants from an informal e-waste

dismantling site, South China. *Environmental Science and Pollution Research*, *22*(2), 1020–1033. https://doi.org/10.1007/s11356-014-3399-1

Wang, T., Zhao, S., Zhu, L., Mcwilliams, J. C., Galgani, L., Amin, R. M., Nakajima, R., Jiang, W., & Chen, M. (2023). *Author Correction: Accumulation, transformation and transport of microplastics in estuarine fronts*. *4*, 419. https://doi.org/10.1038/s43017

Wiesinger, H., Zhanyun Wang, & Stefanie Hellweg. (2021). Deep Dive into Plastic Monomers, Additives, and Processing Aids. *Environmental Science and Technology*, *55*(13), 9339–9351. https://doi.org/10.1021/acs.est.1c00976

Yahyaee, A., Nazifi, M., Kianpour, M., & Heidar, K. T. (2018). Experimental Investigation and Modeling of Activity Coefficient at Infinite Dilution of Solutes Using Dicationic Solvent Based on Pyrrolidinium as a New Stationary Phase in Gas Chromatography. *American Journal of Analytical Chemistry*, *09*(04), 257–271. https://doi.org/10.4236/ajac.2018.94020

Zhang, K., Schnoor, J. L., & Zeng, E. Y. (2012). E-waste recycling: Where does it go from here? *Environmental Science and Technology*, *46*(20), 10861–10867. https://doi.org/10.1021/es303166s

Zhang, L., Liu, J., Liu, H., Wan, G., & Zhang, S. (2015). The occurrence and ecological risk assessment of phthalate esters (PAEs) in urban aquatic environments of China. In *Ecotoxicology* (Vol. 24, Issue 5, pp. 967–984). Kluwer Academic Publishers. https://doi.org/10.1007/s10646-015-1446-4

Zhang, Q., Wang, Z., Xiao, Q., Ge, J., Wang, X., Jiang, W., Yuan, Y., Zhuang, Y., Meng, Q., Jiang, J., Hao, W., & Wei, X. (2023). The effects and mechanisms of the new brominated flame retardant BTBPE on thyroid toxicity. *Food and Chemical Toxicology*, *180*. https://doi.org/10.1016/j.fct.2023.114027

Zheng, J., Mittal, K., Fobil, J. N., Basu, N., & Bayen, S. (2024). Simultaneous targeted and non-targeted analysis of plastic-related contaminants in e-waste impacted soil in Agbogbloshie, Ghana. *Science of the Total Environment*, *917*. https://doi.org/10.1016/j.scitotenv.2024.170219

Zhou, Y., Hou, L., Chen, H., Steenbakkers, R., Sehanobish, K., Wu, P., & Shi, Q. (2017). FT-IR studies of factors affecting the diffusivity of oligo (oxyethylene) fatty acid ester in PE films: Effect of temperature, ethylene oxide chain length and base resin type. *Polymer*, *130*, 150–160. https://doi.org/10.1016/j.polymer.2017.10.001

Zhu, T., Cao, Z., Singh, R. P., Cheng, H., & Chen, M. (2021). In silico prediction of polyethylene-aqueous and air partition coefficients of organic contaminants using linear and nonlinear approaches. *Journal of Environmental Management*, *289*. https://doi.org/10.1016/j.jenvman.2021.112437